ON ALPHA-DECAY IN HEAVY NUCLEI

by

LEONARD RAYMOND SCHERK

B.Sc., University of British Columbia, 1965

A THESIS SUBMITTED IN PARTIAL FULFILMENT OF THE
REQUIREMENTS FOR THE DEGREE OF
MASTER OF SCIENCE

in the department
of
Physics

We accept this thesis as conforming to the
required standard

THE UNIVERSITY OF BRITISH COLUMBIA
March, 1967

In presenting this thesis in partial fulfilment of the requirements for an advanced degree at the University of British Columbia, I agree that the Library shall make it freely available for reference and study. I further agree that permission for extensive copying of this thesis for scholarly purposes may be granted by the Head of my Department or by his representatives. It is understood that copying or publication of this thesis for financial gain shall not be allowed without my written permission.

Department of PHYSICS

The University of British Columbia
Vancouver 8, Canada

Date April 6, 1967

ABSTRACT

The alpha-particle reduced widths for the ground state in Po^{212} are calculated on the basis of the nuclear shell model, employing the technique of Harada, but treating the nuclear surface in a more direct manner. It is contended that the calculations of previous authors, who have generally used a square-edge nucleus and a Coulomb barrier rounded-off by the nuclear potential of Igo, have, essentially, used the equivalent square-edge nucleus model of Vogt. Their J.W.K.B. estimate of the barrier penetrabilities is checked by an analytic calculation in Chapter 3 and is found to be reasonable. It is shown in Chapter 4 that, in the scattering of an alpha-particle from the ground state of Pb^{208}, the diffuse nuclear edge considerably enhances the one-body reduced widths and, in a direct manner, that it similarly enhances the one-body differential elastic scattering cross-section. In this manner, it is demonstrated that the radius involved in the equivalent square-edge nucleus model must be considerably larger than that of the diffuse-edge nucleus to which it corresponds. This is shown directly in Chapter 5, where the validity of the equivalent square-edge nucleus model in heavy nuclei is examined. It is contended that this explains the large radii found in previous calculations. This is demonstrated directly by repeating the calculation of Harada with the diffuse nuclear edge being introduced in a direct manner. Although the effects of configuration mixing have not been directly examined, it has been concluded that shell model

calculations can explain the major part of the empirical decay rates provided that the nuclear surface is treated in a direct manner.

TABLE OF CONTENTS

		Page
CHAPTER 1	INTRODUCTION	1
CHAPTER 2	A DERIVATION OF THE DECAY CONSTANT	7
CHAPTER 3	EXPERIMENTAL REDUCED WIDTHS	21
3-1	THE REACTION $Po^{212} \longrightarrow Pb^{208} + \alpha$	22
3-2	COMPARISONS WITH J.W.K.B. AND SQUARE-WELL ESTIMATES	24
CHAPTER 4	INDEPENDENT-PARTICLE MODEL DECAY RATES OF Po^{212}	29
4-1	ONE-BODY REDUCED WIDTHS AND EXPERIMENTAL SPECTROSCOPIC FACTORS	32
4-2	ONE-BODY DIFFERENTIAL ELASTIC SCATTERING CROSS-SECTION OF Pb^{208} FOR AN ALPHA-PARTICLE AT 90°_{CM}	41
4-3	HARADA'S FORMULA FOR THE INDEPENDENT-PARTICLE MODEL REDUCED WIDTHS	43
4-4	NUMERICAL INDEPENDENT-PARTICLE MODEL REDUCED WIDTHS	47
CHAPTER 5	THE EQUIVALENT SQUARE-EDGE NUCLEUS MODEL	52
5-1	THE EQUIVALENT SQUARE-EDGE NUCLEUS MODEL	53
5-2	APPLICATIONS TO HEAVY NUCLEI	54
CHAPTER 6	CONCLUSIONS	62
	BIBLIOGRAPHY	65
APPENDIX A	HARADA'S FORMULA FOR THE REDUCED WIDTH FOR ALPHA-PARTICIE DECAY IN EVEN-EVEN NUCLEI	66
APPENDIX B	TALMI TRANSFORMATION COEFFICIENTS	74
APPENDIX C	CALCULATION OF THE ONE-BODY DIFFERENTIAL ELASTIC SCATTERING CROSS-SECTION	80

LIST OF TABLES

		Page
TABLE 1	EXPERIMENTAL REDUCED WIDTHS	25
TABLE 2	ONE-BODY POTENTIALS	37
TABLE 3	EXPERIMENTAL SPECTROSCOPIC FACTORS	38
TABLE 4	OVERLAP INTEGRALS	49
TABLE 5	COMPARISON OF DECAY RATES	50
TABLE 6	CALCULATED SPECTROSCOPIC FACTORS	50

LIST OF FIGURES

		Page
FIGURE 1	SURFACE POTENTIAL (Pb^{208})	26
FIGURE 2	COMPARISON OF DECAY-RATE PARAMETERS WITH SQUARE-WELL AND J. W. K. B. ESTIMATES (Pb^{208})	27
FIGURE 3	SQUARE AND DIFFUSE POTENTIALS (Pb^{208})	34
FIGURE 4	RESONANT WAVE FUNCTIONS FOR SQUARE AND DIFFUSE POTENTIALS (Pb^{208})	35
FIGURE 5	RESONANT WAVE FUNCTIONS: EFFECT OF WELL DEPTH	39
FIGURE 6	RESONANT WAVE FUNCTIONS: EFFECT OF SURFACE THICKNESS	40
FIGURE 7	ONE-BODY SCATTERING CROSS-SECTION (Pb^{208})	42
FIGURE 8	BARRIER ABSORPTION (Pb^{208})	59
FIGURE 9	REFLECTION FACTOR (Pb^{208})	60

ACKNOWLEDGEMENTS

I wish to thank Professor E. W. Vogt for his continual encouragement and generous assistance in the solution of this problem. This thesis was done while the author was supported by a bursary from the National Research Council of Canada.

CHAPTER 1 INTRODUCTION

The aim of this thesis is to estimate the extent to which the independent-particle model can explain alpha-particle decay rates in heavy nuclei. A considerable amount of earlier work has had this aim (c.f. Mang (1964)), but past estimates of the alpha-particle decay rates have tended to be smaller than the observed decay rates. The calculated rates are a product of two factors: a) a spectroscopic factor, which accounts for the many-body aspects of the nuclear problem; b) a one-body decay constant, which accounts for the average interaction of the alpha-particle with the daughter nucleus. We find that much of the remaining discrepancy between the calculated and the observed decay rates can be removed by a more direct and more accurate treatment of the nuclear surface in the calculation of the one-body decay constant. We will demonstrate that, apart from a difference in their reflection properties, a heavy nucleus having a diffuse-edge behaves like a considerably larger nucleus having a square-edge in the analysis of alpha-particle decay rates or alpha-particle scattering cross-sections. (The decay rates are related to the scattering cross-sections in a simple manner; the decay constant is proportional to the width of the elastic scattering cross-section.)

Vogt (1962) has suggested that one may, in general, replace a conventional diffuse-edge nucleus with an "equivalent square-edge nucleus" which he defines in the following manner. He considers a simple one-body model in which the incident

particle is scattered by a potential well. This is the nuclear problem without the many-body aspects; in fact, the spectroscopic factor (which accounts for the many-body aspects of the problem) is rather insensitive to the nature of the nuclear surface and to the size of the nucleus. He replaces the diffuse-edge nuclear potential well with an "equivalent square-edge well" whose radius and depth are chosen so that it exhibits a resonance at the resonance energy of the diffuse-edge well and so that the resonant wave function of the square-edge well satisfies the following conditions: a) it has the same number of nodes as the resonant wave function of the diffuse-edge well; b) it has the same amplitude as the resonant wave function of the diffuse-edge well at the radius of the square-edge well. Now the one-body scattering width (or decay constant) is a product of two factors: a) a one-body reduced width, which depends only upon the amplitude of the resonant wave function at the nuclear radius (and, hence, on the internal aspects of the nucleus); b) a penetrability, which depends only upon the reflective properties of the potential barrier outside of the nuclear radius. Apparently the only difference in the one-body problem between the diffuse-edge well and the corresponding equivalent square-edge well is the anomalous reflection of the latter; this difference in reflection is assigned to a "reflection factor".

Vogt (1962) has found for neutron scattering, and Vogt, Michaud, and Reeves (1965) for alpha-particle scattering from light nuclei, that the equivalent square-edge well has a con-

siderably larger radius than the corresponding diffuse-edge well; in general, it has about the same depth as the diffuse-edge well and the reflection factor is found to be small. In fact, the parameters of the equivalent square-edge well are found to be rather insensitive to the nature of the reaction and to the many-body aspects of the problem so that the diffuse-edge nucleus does behave like a larger square-edge nucleus. In this thesis, we will show that these results apply to the alpha-particle decay rates of heavy nuclei; in fact, we will show that the previous calculations have generally used this equivalent square-edge well, thus hiding the true radius of the decay problem.

It is of considerable value to show that the discrepancies between the empirical and the calculated alpha-particle decay rates found in the earlier calculations have lain in the method of calculation rather than in the independent-particle model assumptions. The failure of the independent-particle model would imply that the model does not introduce sufficient correlations into the nuclear wave functions to account for the observed clustering into alpha-particles. The fact that the Pauli Exclusion Principle becomes less inhibitive in the surface region makes it seem natural to attribute much of the clustering to the nuclear surface. Wilkinson (1961) has interpreted the discrepancy between the empirical and calculated alpha-particle decay rates as evidence that one cannot easily describe the nuclear wave function in the surface region by shell-model wave functions; in fact, he has suggested that

it might be necessary to resort to a phenomenological cluster model. A natural way in which to introduce correlations into the independent-particle model wave functions is through configuration mixing; Harada (1961) and Zeh and Mang (1962) have found this enhances the calculated decay rates by an order of magnitude. We contend that the remaining discrepancy between the empirical and the calculated decay rates can be removed by a correct interpretation of the radius involved in the calculations.

The procedure used in calculating the alpha-particle decay rates is familiar from the theory of nuclear reactions. In Chapters 2 and 3 of this thesis, we have derived a formula for the decay constant by this procedure. However, we have developed the decay constant from a point of view which is appropriate to the decay problem rather than to the scattering problem. The formula for the decay constant has been developed in this manner by several other authors, particularly Zeh (1963) and Mang (1964).

Igo (1959) has used the elastic scattering data to empirically determine the modification of the Coulomb fields in the nuclear surface by the real, average interaction of an alpha-particle with a heavy nucleus. We use Igo's nuclear potential to round off the Coulomb barriers. The penetrability through a rounded-off Coulomb barrier can be determined quite easily and, in Chapter 3, the penetrability is evaluated for either the scattering of an alpha-particle from Pb^{208} or of its decay from Po^{212}. The results are compared with those obtained from

the J.W.K.B. and square-well estimates; the latter estimates have been used in most of the previous calculations.

We have previously noted that most of the effects of the nuclear surface upon the alpha-particle decay rates are assigned to the one-body decay constants rather than to the spectroscopic factors. In Chapter 4, we investigate the effect of the nuclear surface upon the one-body decay constants. By comparing the resonant wave function of a diffuse-edge nucleus with that of a square-edge nucleus of the same radius, we show that the diffuse-edge enhances the reduced widths of the one-body problem. In fact, it is seen from these resonant wave functions that the diffuse-edge nucleus corresponds to a considerably larger equivalent square-edge nucleus. This suggests that the one-body scattering cross-sections should be considerably enhanced by the diffuse-edge; in fact, we show this in a direct manner by calculating the differential elastic scattering cross-section for the scattering of an alpha-particle from a potential well appropriate to a Pb^{208} nucleus.

We include the many-body aspects of the decay problem by repeating the independent-particle model calculation of Harada (1961) for the alpha-particle decay rate of Po^{212}. Harada has used a square-edge well of radius ten fermis to to evaluate the amplitude of the one-body resonant wave functions; he has rounded-off the Coulomb barrier with the nuclear potential of Igo (1959). He has chosen his model wave functions to be infinite harmonic oscillator wave functions and has determined the harmonic oscillator size parameter by

taking the amplitude of the mode of the relative motion to be equal to the amplitude of the one-body square-well wave functions. While it is not obvious that this procedure really represents a square-well calculation, it might be suspected that it does since the effects of the internal modes are rather insensitive to the size parameter. The radius of Harada's calculation is considerably larger than those believed typical of heavy nuclei; in fact, we contend that he has essentially used the equivalent square-edge well of a smaller diffuse-edge well. In Chapter 4, we repeat his calculation but replace the one-body wave functions of the square-edge well with the one-body wave functions of a smaller diffuse-edge well. We show that the decay constant obtained in this manner for Po^{212} is comparable to that which Harada has obtained with the larger square-edge well. In fact, we calculate the equivalent square-edge well of a typical diffuse-edge well in Chapter 5 and find that the difference in the radii of the two wells is similar to that found in the preceding decay rate calculations.

In addition to discussing alpha-particle decay, we use the barrier penetration calculations to study absorption processes. In Chapter 5, we give the extent to which the equivalent square-well model is found to apply to the alpha-particle absorption of a Pb^{208} nucleus. The effect of the strength of the optical model potential in the electrostatic barrier is also studied.

A summary of the preceding calculations is given in Chapter 6.

CHAPTER 2 A DERIVATION OF THE DECAY CONSTANT

The systems which will be discussed in this thesis are nuclear systems which decay by means of simple alpha-particle disintegration. The formalism for describing such systems is familiar from the theory of nuclear reactions; in fact, Thomas (1954) has derived the decay constant of such a system by the standard techniques of nuclear reaction theory. The purpose of the derivation provided in this thesis is to employ these techniques in a similar manner, but from a point of view which is more natural to the study of decay problems.

The most obvious method in which to describe a decaying system would be to find the wave function of the system at some convenient time, say t_0. If at this time it is found that the system is described by the quantum numbers, $\eta(t_0)$, then the temporal evolution of the system is governed by the Schroedinger Equation;

$$(2.1) \qquad i\hbar \frac{d}{dt} |\eta(t)\rangle = H|\eta(t)\rangle .$$

(Here H is the Hamiltonian of the system and $\hbar$ is the crossed Planck's constant.)

A natural choice for t_0 would be at a time prior to the formation of the system. If t_0 were chosen sufficiently negative, one could think of the system as consisting of the wave packets of the constituent particles, with negligible overlap and interacting through slowly varying potentials, and as converging on the point at which the system formed; the dynamics of the wave packets (at the speeds of interest) are then Newtonian so that $|\eta(t_0)\rangle$ may be determined precisely.

The difficulty in this modus operandi is that, after having converged and formed, the system does not decay for a time many orders of magnitude longer than the typical period of a constituent nucleon's motion within the formed system. The temporal fluctuations of the wave function of the formed system, which at first were strongly correlated to the formation process, after a time become statistical.

It is, therefore, more expedient to choose t_o after the formation process and to construct a statistically determined wave function of the constituent nucleons, the nucleons being assumed to be within the nuclear volume. In practice, it may be hoped to realize this statistical distribution by forming the nuclear wave functions from models such as the independent-particle model. For this reason, the wave function of the formed state is commonly referred to as the "parent nucleus" wave function.

Care must be exercised in interpreting this stationary state approximation. Such stationary wave functions are irregular at infinity, while the parent nucleus wave function is not only regular at infinity but essentially vanishes outside the nuclear radius. Therefore, the approximation is useful only within the volume of the formed system.

Assuming a parent nucleus at t = 0, and assuming two fragment break-up, it would seem reasonable to choose the wave function of the decaying system to be of the form,

$$\Psi(\underline{x}_1,\underline{s}_1,\underline{x}_2,\underline{s}_2,\ldots,\underline{x}_A,\underline{s}_A,t) = \cdots$$

$$\cdots = a(t)\Psi_o(\underline{x}_1,\underline{s}_1,\underline{x}_2,\underline{s}_2,\ldots\underline{x}_A,\underline{s}_A) + \cdots$$

$$\cdots + \sum_{c_1,c_2}\int d\epsilon\, b_{c_1c_2}(\epsilon,t)\,\psi_{c_1}(q_1^i)\psi_{c_2}(q_2^j)\phi_{c_1c_2}(\underline{R},t), \tag{2.2}$$

where

$$\Psi_o(\underline{x}_1,\underline{s}_1,\underline{x}_2,\underline{s}_2,\ldots,\underline{x}_A,\underline{s}_A) = \cdots$$

$$\cdots = \Psi(\underline{x}_1,\underline{s}_1,\underline{x}_2,\underline{s}_2,\ldots,\underline{x}_A,\underline{s}_A,0),$$

and where $(\underline{x}_i,\underline{s}_i)$ are the spatial and spin co-ordinates of the i^{th} nucleon, respectively. Here, $\psi_{c_1}(q_1^i)$ and $\psi_{c_2}(q_2^j)$ are the wave functions of the first and second decay fragments; c_1 and c_2 are the appropriate quantum numbers. $\phi_{c_1c_2}(\underline{R},\epsilon)$ is a stationary state of the relative motion; ϵ is the relative energy and $\underline{R}$ the separation of the fragments.

A theory of alpha-decay has been developed from this point of view by Mang (1960). In applications to the alpha-decay of heavy nuclei, he finds that,

$$(2.3)\quad a(t) \doteq \mathrm{EXP}\left(-\frac{i}{\hbar}(\epsilon - i\gamma)t\right).$$

In fact, the formula which he obtains for γ is essentially the same as that which will be obtained in the calculation to be discussed.

At large positive times, the parent nucleus will have decayed and should be describable as an alpha-particle and a daughter nucleus at some large relative separation. Zeh (1963) has noted that, in a suitably small space-time region, the time dependence of the parent nucleus wave function may be taken to be that of Eq. (2.3) and the wave functions in each channel of break-up,

$$(2.4)\quad G_{c_1c_2}(\underline{R},t) = \langle c_1c_2\underline{R}|\eta(t)\rangle,$$

may be taken to be those of purely outgoing flux. In this thesis we shall follow this approach. The parent nucleus wave function will be expanded in the nuclear volume in terms

of a complete set of stationary states which explicitly include the alpha-decay channels; the boundary conditions at the nuclear radius will be chosen so that the channel wave functions are asymptotically waves of outgoing flux. To determine the required expansion coefficients, it will be assumed that the parent nucleus wave function can be described by the independent-particle model. Of course, this procedure is well-known and has often been used in the analysis of nuclear reactions.

In the construction of the parent nucleus wave function, it will be assumed that non-local and many-body potentials can be neglected and that the Hamiltonian of the system, which will be assumed to consist of A nucleons (N neutrons and Z protons), can be written in the form,

$$(2.5) \qquad H = \sum_{i=1}^{A} H_i ,$$

where,

$$(2.6) \qquad H_i = -\frac{\hbar^2}{2m}\nabla^2_{\underline{x}_i} + \tfrac{1}{2}\sum_{j=1}^{A} V_{ij}(\nu_i, \nu_j).$$

Here,

$$\nu_i = (\underline{x}_i, s_i),$$

are the spatial and spin co-ordinates, respectively, of the i^{th} nucleon; the proton and neutron masses have been assumed to be equal.

The construction of the independent-particle model wave functions is well-known (Preston (1962)). One calculates the spatial average of the potential term in Eq. (2.6) at the i^{th} nucleon; from this average potential one derives the one-nucleon orbitals. The parent nucleus wave function is then formed of linear combinations of the Slater Determinants of

the assumed configuration; the linear combinations are chosen appropriate to the quantum numbers of the parent nucleus. The residual interaction does not, in general, vanish; if it can be treated as a small perturbation, one can introduce the resultant mixing of the configurations by the techniques of perturbation theory.

To find the nature of the stationary states of the Hamiltonian commensurate with the system after decay, it is desirable to introduce the approximations in a manner convenient for constructing alpha-particle and daughter nucleus wave functions. In the discussion of this chapter, it will be assumed that the alpha-particle and daughter nucleus wave functions have been antisymmetrized with respect to the interchange of proton or of neutron co-ordinates; the parent nucleus wave function to be constructed from these wave functions will, therefore, only be partially antisymmetrized. However, it will be shown that the parent nucleus wave function can be regarded as a solution of a Schroedinger Equation having a complex eigenvalue (Eq. (2.25)). Since the Hamiltonian is symmetric in the interchange of the co-ordinates of any two identical particles, the completely antisymmetrized wave function will be an eigenstate of the above Schroedinger Equation if the partially antisymmetrized wave functions are solutions. Only the latter fact will be used in the arguments to follow.

It will be assumed that the system of nucleons labelled by (1234) constitutes the alpha-particle, where 1 and 2 are protons and 3 and 4 are neutrons; the remaining nucleons,

(56...A), will be taken as constituting the daughter nucleus. It is convenient to make the definitions,

$$\underline{x}_\alpha = (\underline{x}_1, \underline{x}_2, \underline{x}_3, \underline{x}_4); \qquad \underline{x}_\sigma = (\underline{x}_5, \underline{x}_6, \ldots, \underline{x}_A);$$

$$\underline{s}_\alpha = (\underline{s}_1, \underline{s}_2, \underline{s}_3, \underline{s}_4); \qquad \underline{s}_\sigma = (\underline{s}_5, \underline{s}_6, \ldots, \underline{s}_A);$$

and to introduce the relative co-ordinates,

$$(2.7)\quad \underline{R}_\alpha = \tfrac{1}{4}(\underline{x}_1 + \underline{x}_2 + \underline{x}_3 + \underline{x}_4); \quad \underline{R}_\sigma = \frac{1}{A-4}(\underline{x}_5 + \underline{x}_6 + \cdots + \underline{x}_A);$$

$$\underline{R}_{CM} = \frac{1}{A}(\underline{x}_1 + \underline{x}_2 + \cdots + \underline{x}_A); \quad \underline{\xi}_1 = \underline{x}_1 - \underline{x}_2;$$

$$\underline{\xi}_2 = \underline{x}_3 - \underline{x}_4; \quad \underline{\xi}_3 = \tfrac{1}{2}(\underline{x}_1 + \underline{x}_2) - \tfrac{1}{2}(\underline{x}_3 + \underline{x}_4);$$

$$\underline{\xi} = (\underline{\xi}_1, \underline{\xi}_2, \underline{\xi}_3); \quad \underline{R} = \underline{R}_\alpha - \underline{R}_\sigma .$$

(The Jacobian of the transformation $(\underline{x}_1, \underline{x}_2, \underline{x}_3, \underline{x}_4) \longrightarrow (\underline{R}_\alpha, \underline{\xi}_1, \underline{\xi}_2, \underline{\xi}_3)$ is unity.)

After decay, the nuclear system can be described by a "one-body" model; by this we mean that the interaction between the daughter nucleus and the alpha-particle is a function only of their separation. If the calculations are performed in the center-of-mass frame,

$$-\frac{\hbar^2}{2(Am)} \nabla^2_{\underline{R}_{CM}} \Psi = 0,$$

and if A is sufficiently large that the recoil in the daughter nucleus wave function can be neglected,

$$-\frac{\hbar^2}{2(A-4)m} \nabla^2_{\underline{R}_\sigma} \Psi = 0,$$

then one can write,

$$(2.8)\quad H = H_\alpha + H_\sigma + H_{\alpha\sigma},$$

where,

$$(2.9)\ a)\quad H_\alpha = \sum_{i=1}^{3} -\frac{\hbar^2}{2\mu_i} \nabla^2_{\underline{\xi}_i} + \tfrac{1}{2} \sum_{i=1}^{4} \sum_{j=1}^{4} V_{ij}(r_i, r_j);$$

$$b)\quad H_\sigma = \sum_{i=5}^{A} -\frac{\hbar^2}{2m} \nabla^2_{\underline{x}_i} + \tfrac{1}{2} \sum_{i=5}^{A} \sum_{j=5}^{A} V_{ij}(r_i, r_j);$$

c) $H_{rel} = -\frac{\hbar^2}{2\mu}\nabla^2_{\underline{R}} + U(\underline{R})$.

Here,

(2.10) $\mu = \frac{4(A-4)}{A}\,m$; $\mu_1 = \mu_2 = \frac{m}{2}$; $\mu_3 = \frac{m}{4}$;

are the reduced masses with respect to the relative co-ordinates $\underline{R}$, $\underline{\xi}_1$, $\underline{\xi}_2$, and $\underline{\xi}_3$, respectively; $U(\underline{R})$ represents the average interaction between the decay fragments.

The effect of the residual interaction between the decay fragments can be accounted for by taking $U(\underline{R})$ to be an optical model potential:

(2.11) $U(\underline{R}) = V(\underline{R}) + iW(\underline{R})$. (V and W are real.)

It is well-known that the complex term, $W(\underline{R})$, simulates many of the effects of the residual interaction; it essentially vanishes outside of the nuclear volume. In practice, both $V(\underline{R})$ and $W(\underline{R})$ are regarded as being phenomenological; in general, they will be dependent upon the relative energy of the decay fragments and upon the channels being considered. We will neglect this dependence.

In this thesis, we will be concerned only with the spherical nucleus, Pb^{208}. $U(\underline{R})$ then depends only upon the distance between the decay fragments so that the states of relative motion are solutions of the Schroedinger Equation,

(2.12) $(-\frac{\hbar^2}{2\mu}\nabla^2_{\underline{R}} + U(R))\psi(\underline{R}) = \epsilon\psi(\underline{R})$.

The solutions of Eq. (2.12) have the form,

(2.13) $\psi(\underline{R}) = \frac{U_L(R)}{R}\; Y_L^{M_L}(\frac{\underline{R}}{R})$,

where $Y_L^{M_L}(\frac{\underline{R}}{R})$ is a spherical harmonic and $U_L(R)$ is a solution of the radial Schroedinger Equation,

(2.14) $-\frac{\hbar^2}{2\mu}\frac{d^2}{dR^2}u_L(R) + (U(R) + \frac{\hbar^2}{2\mu}\frac{L(L+1)}{R^2})\,u_L(R) = \cdots$

$\cdots = \epsilon_L\, u_L(R)$.

The eigenstates of the total Hamiltonian, H, are then of the form,

$$(2.15)\quad \psi_{\alpha\sigma LM_L} = \psi^{\gamma_\alpha}_{j_\alpha m_\alpha}(\underline{\xi}, \underline{s}_\alpha)\, \psi^{\gamma_\sigma}_{j_\sigma m_\sigma}(\underline{x}_\sigma, \underline{s}_\sigma)\frac{u_L(R)}{R}\, Y_L^{M_L}\left(\frac{R}{R}\right),$$

where $\psi_{j_\alpha m_\alpha}$ and $\psi^{\gamma_\sigma}_{j_\sigma m_\sigma}$ are standard eigenstates of the angular momenta, j_α and j_σ, respectively, and are solutions of the Schroedinger Equations,

$$(2.16)\ a)\quad H_\alpha \psi^{\gamma_\alpha}_{j_\alpha m_\alpha} = E^{\gamma_\alpha}_{j_\alpha} \psi^{\gamma_\alpha}_{j_\alpha m_\alpha};$$

$$b)\quad H_\sigma \psi^{\gamma_\sigma}_{j_\sigma m_\sigma} = E^{\gamma_\sigma}_{j_\sigma} \psi^{\gamma_\sigma}_{j_\sigma m_\sigma}.$$

γ_α and γ_σ are the remaining quantum numbers required to specify the states completely.

The many-body aspects of the decay problem are contained within the nuclear volume. For the purposes of analyzing alpha-decay rates, it is convenient to define a set of functions in the following manner. In each channel, one can define a boundary condition number, b_c;

$$(2.17)\quad \left(R\,\frac{d\,u^c(R)}{dR} + u^c(R)\right)\Big|_{R=R_0} = b_c\ .$$

Here, R_0 is taken as the radius of the parent nucleus; the functions, $u^c(R)$, are taken to be normalized in $R \leq R_0$. (We will later show that the boundary conditions can be chosen in a manner which is natural to the decay problem.) These boundary conditions, together with the differential equation, Eq. (2.14), yield a set of solutions of Eq. (2.14) which are complete within $R < R_0$. These solutions may be taken to be, $u^c_n(R)$, where n is the number of nodes of u^c_n. Since the solutions of Eq. (2.16) (which are defined over all space) are complete, one can define a complete set of functions in the following manner. One defines the channel wave function

to be,

$$(2.18)\quad \psi_c = \frac{1}{R_0}\,\psi^{\tau_\alpha}_{j_\alpha m_\alpha} \sum_{m_\sigma M_L} \langle j_\sigma L\, m_\sigma M_L \mid JM\rangle\, \psi^{\tau_\sigma}_{j_\sigma m_\sigma} Y_L^{M_L},$$

where c denotes the channel quantum numbers, $(j_\alpha, m_\alpha, \tau_\alpha, j_\sigma, \tau_\sigma, L, J, M)$. The set of functions,

$$(2.19)\quad \psi_{nc} = u_n^c\,\psi_c,$$

is then complete within $R \geq R_0$ so that one can make the expansion,

$$(2.20)\quad \Psi_o = \sum_{n,c} c_{nc} u_n^c \psi_c,$$

where,

$$(2.21)\quad c_{nc} = \int\!\!\int_{\mathcal{V}} \Psi_o\, u_n^{c*} \psi_c^*\, d\mathcal{V}.$$

Nuclear systems exhibiting alpha-decay typically have long lifetimes whence it might be expected that they should, in some sense, behave like a stationary state. To see in what sense this is true, it will be assumed that the coefficients, $a(t)$ and $b_{c_1c_2}(\epsilon,t)$ of Eq. (2.2), are of the form,

$$(2.22)\quad a(t) = \mathrm{EXP}(-\tfrac{i}{\hbar} E_o t)\mathrm{EXP}(-\tfrac{\gamma}{\hbar} t);$$

$$b_{c_1c_2}(\epsilon,t) = \mathrm{EXP}(\tfrac{i}{\hbar} E_o t)\,(1 - \mathrm{EXP}(-\tfrac{\gamma}{\hbar} t) b_{c_1c_2}(\epsilon).$$

(This temporal dependence has, in fact, been justified from theoretical considerations by Mang (1960).) Accepting Eq.(2.22), the time-dependent wave function is of the form,

$$(2.23)\quad \Psi(t) = \mathrm{EXP}(-\tfrac{i}{\hbar} E_o t)\,(\Psi_o\, \mathrm{EXP}(-\tfrac{\gamma}{\hbar} t) \quad \cdots$$

$$\cdots \quad (1 - \mathrm{EXP}(-\tfrac{\gamma}{\hbar} t)\,\Psi_d),$$

where Ψ_d represents the system after decay. The Schroedinger Equation of the system then becomes,

$$(2.24)\quad i\hbar\frac{\partial\Psi(t)}{\partial t} = (E_o - i\gamma)\Psi(t) + i\gamma\mathrm{EXP}(-\tfrac{i}{\hbar} E_o t)\Psi_d = H\Psi(t).$$

Since γ is, in general, small, a good approximation to the

parent nucleus wave function should be obtained by solving the complex eigenvalue problem,

$$(2.25)\quad H\Psi_o = (E_o - i\gamma)\Psi_o .$$

Written in the form,

$$(H + i\gamma)\Psi_o = E_o\Psi_o ,$$

it is seen that γ can be treated as a perturbation with the zeroth order approximation of Eq. (2.25) being a stationary state.

From Eq. (2.25),

$$(2.26)\quad -2i\gamma|\Psi|_o^2 = \Psi_o^* H\Psi_o - \Psi_o H\Psi_o^* .$$

Defining the decay constant by,

$$(2.27)\quad \lambda = \frac{2\gamma}{\hbar} ,$$

employing Eq. (2.9) and Green's Theorem, and integrating Eq. (2.26) over all space,

$$(2.28)\quad \lambda = \frac{i}{\hbar}\int_0^{R_o}\int_{\Omega_\xi, \underline{x}_\sigma, \underline{s}} (\Psi_o^* H\Psi_o - \Psi_o H\Psi_o^*)R^2 dR d\underline{\xi}\, d\underline{x}_\sigma\, d\underline{s}\, d\Omega$$

$$= (1) \sum_{\substack{n, j_\sigma, \tau_\sigma \\ L, J, M}} \int_{\underline{s}_\alpha}\int_{\Omega_\xi \to \infty} \mathrm{Real}\Big(\sum_{j_\alpha, m_\alpha, \tau_\alpha} C_{n j_\alpha m_\alpha \tau_\alpha j_\sigma \tau_\sigma LJM}\psi^{\tau_\alpha}_{j_\alpha m_\alpha}\Big)^*$$

$$\cdots x\Big(\sum_{i=1}^{3}\frac{\hbar}{i\nu_i}\nabla_{\xi i}\Big)x\Big(\sum_{j_\alpha', m_\alpha', \tau_\alpha'} C_{n j_\alpha' m_\alpha' \tau_\alpha' j_\sigma \tau_\sigma LJM}\psi^{\tau_\alpha'}_{j_\alpha' m_\alpha'}\Big)$$

$$\cdots x\, d\Omega_\xi\, d\underline{s}_\alpha$$

$$(2)\sum_{\substack{n, j_\alpha, m_\alpha \\ L, M_L, \tau_\alpha}} \int_{\underline{s}_\sigma}\int_{\Omega_{\underline{x}_i}\to\infty} \mathrm{Real}\Big(\sum_{\substack{j_\sigma, \tau_\sigma \\ J, M}} C_{n j_\alpha m_\alpha \tau_\alpha j_\sigma \tau_\sigma LJM}$$

$$\cdots x\sum_{m_\sigma}\langle j_\sigma Lm_\sigma M_L | JM\rangle\psi^{\tau_\sigma}_{j_\sigma m_\sigma}\Big)^* x\Big(\sum_{i=5}^{A}\frac{\hbar}{im}\nabla_{\underline{x}_i}\Big)$$

$$\cdots x\sum_{\substack{j_\sigma', \tau_\sigma' \\ J', M'}} C_{n j_\alpha m_\alpha \tau_\alpha j_\sigma' \tau_\sigma' LJ'M'}\sum_{m_\sigma'}\langle j_\sigma' Lm_\sigma' M_L | JM\rangle$$

$$\cdots x\,\psi^{\tau_\sigma'}_{j_\sigma' m_\sigma'})\, d\Omega_{\underline{x}}\, d\underline{s}_\sigma$$

$$(3)\quad \sum_c \text{Real}\left[\left(\sum_n C_{nc}u_n^c\right)^{*}x\left(\frac{\hbar}{i\nu}\frac{d}{dR}\right)x\left(\sum_{n'} C_{n'c}u_{n'}^c\right)\right]_{R=R_0}.$$

Eq. (2.28) is of the form,

$$\lambda = (1)\sum_{\substack{n,j_\alpha,\tau_\alpha,\\ L,J,M}} \int_{\xi\to\infty} i_{n j_\alpha \tau_\alpha LJM}\, d\mathcal{S}_\xi$$

$$(2)\sum_{\substack{n,j_\alpha,m_\alpha,\\ \tau_\alpha,L,M_L}} \int_{x_\alpha\to\infty} i_{n j_\alpha m_\alpha \tau_\alpha LM_L}\, d\mathcal{S}_{x_\alpha}$$

$$(3)\sum_c \int_{|R|=R_0} i_c^{\alpha\sigma}\cdot d\Omega,$$

where i denotes the probability current in the specified channels. For heavy alpha-emitters, decay through channels other than simple alpha-decay is generally negligible so that terms (1) and (2) in Eq. (2.28) can be neglected. Eq. (2.28) can then be written in the form,

$$(2.29)\quad \lambda = -\frac{i\hbar}{2\mu}\sum_{c,n,n'} C_{nc}^{*}C_{n'c}\left(u_n^{c*}\frac{du_{n'}^c}{dR} - u_{n'}^c\frac{du_n^{c*}}{dR}\right)\Big|_{R=R_0}.$$

A natural choice of the boundary conditions is to match the radial wave functions in each channel onto the wave of purely outgoing flux in that channel. This is accomplished by choosing,

$$(2.30)\quad b_c = S_c(\epsilon_c,R_0) + iP_c(\epsilon_c,R_0);\ (\epsilon_c = E_0 - E_{j_\alpha}^{\tau_\alpha} - E_{j_\beta}^{\tau_\beta})$$

S_c and P_c are the nuclear shift function and the nuclear penetrability:

$$(2.31)\quad S_c(\epsilon_c,R_0) + iP_c(\epsilon_c,R_0) = \cdots$$

$$\cdots = R\cdot\left.\frac{\bar{G}_c'(\epsilon_c,R) + i\bar{F}_c'(\epsilon_c,R)}{\bar{G}_c(\epsilon_c,R) + iF_c(\epsilon_c,R)}\right|_{R=R_0}.$$

Here $\bar{F}_c$ and $\bar{G}_c$ are those solutions of Eq. (2.14) which are asymptotic to the regular and irregular Coulomb functions, F_c and G_c, in the channel c. (The one-body potential is essen-

tially the Coulomb potential outside of the nuclear surface.)

The optical model potential, U(R), is essentially phenomenological. Its behaviour in the nuclear surface has been determined from the elastic scattering data by Igo (1959), but the depth of the real and imaginary terms within the nuclear volume is largely arbitrary. (Values of 100-150 MEV for V(R) and 5-10 MEV for W(R) are currently fashionable.) To the extent that the residual interaction can be neglected, we need only retain the real term, V(R), in Eq. (2.14). It would then seem natural to choose the depth of the well in such a manner that, for some n_o,

$$(2.32)\quad \epsilon^c_{n_o} = \epsilon_c \ .$$

This one-body wave function should then represent many of the radial properties of the actual wave function of the decaying system. (The arbitrariness in the number of nodes reflects the ignorance of the well depth.)

The one-body reduced width, $|\gamma^c_n|^2$, is defined by,

$$(2.33)\quad \gamma^c_n = \sqrt{\frac{\hbar^2}{2\mu R_o}}\, u^c_n(R_o),$$

By noting the boundary condition, Eq. (2.30), Eq. (2.29) can be written in the form,

$$(2.34)\quad \lambda = \sum_c \frac{2P_c(\epsilon^c_{n_o}, R_o)\,|\gamma^c_{n_o}|^2}{\hbar} \sum_{n,n'} C^*_{nc} C_{n'c} \frac{\gamma^{c\,*}_n \gamma^c_{n'}}{|\gamma^c_{n_o}|^2} \ .$$

Defining the one-body decay constants,

$$(2.35)\quad \lambda^{o.b.}_c = \frac{2P_c(\epsilon^c_{n_o}, R_o)\,|\gamma^c_{n_o}|^2}{\hbar} \ ,$$

and the spectroscopic factors,

$$(2.36)\quad S_c = \left| \sum_n C_{nc} \frac{\gamma^c_n}{\gamma^c_{n_o}} \right|^2 \ ,$$

Eq. (2.34) can be written in the form,

$$(2.37)\quad \lambda = \sum_c \lambda_c^{o.b.} S_c .$$

Eq. (2.37) is convenient for calculations of the decay constant from the nuclear models.

It is seen from Eq. (2.25) that we may approximate the parent nucleus wave function, Ψ_o, by X_o, where X_o is the familiar resonant state of reaction theory defined by,

$$(2.38)\quad HX_o = E_o X_o .$$

It is a result of reaction theory that the width of the elastic scattering cross-section (as determined by the Breit-Wigner single-level resonance formula) is,

$$(2.39)\quad \Gamma_{oc} = \sum_c \lambda_{oc}^{o.b.} S_c ,$$

where S_c is the spectroscopic factor of Eq. (2.36) and $\lambda_{oc}^{o.b.}$ is the one-body width,

$$(2.40)\quad \Gamma_{oc}^{o.b.} = 2P_c(\epsilon_{n_o}^c, R_o)\left|\gamma_{no}^c\right|^2 .$$

Comparing Eq. (2.40) and Eq. (2.35),

$$(2.41)\quad \Gamma_{oc} = \lambda \hbar ,$$

which is an expression of the Uncertainty Principle.

If the residual interaction is sufficiently small, then only the one-body wave functions, $u_{n_o}^c$, are contained appreciably in the parent nucleus wave function. Eq. (2.36) then reduces to,

$$(2.42)\quad S_c = \left|C_{n_o c}\right|^2 ,$$

and Eq. (2.37) to,

$$(2.43)\quad \lambda = \sum_c \lambda_c^{o.b.} \left|C_{n_o c}\right|^2 .$$

To test the validity of the one-body model, we note that many of the effects of the residual interaction can be accounted for by the optical model potential (Eq. (2.11)). The absorp-

tion cross-section for such a potential is of the form,

$$(2.44)\quad \sigma_{abs} = \frac{\pi}{k_c^2} \sum_L g_c T_c; \qquad (k_c = \sqrt{\frac{2\mu\epsilon_c}{\hbar}})$$

T_c is the optical model transmission function in the channel, c; L is the relative angular momentum in the channel, c; g_c is a numerical factor depending on the angular momenta of the parent nucleus, the daughter nucleus, and the alpha-particle. If W_o is taken as the order of magnitude of the depth of the complex part of the optical model potential, then, in the one-body approximation about E_o, the transmission function is of the form,

$$(2.45)\quad T_c(E) \doteq 4P_L(\epsilon_L, R_o)\, c_L \frac{\hbar^2}{\mu R_o^2} \frac{W_o}{(E - \epsilon^c_{n_o})^2 + W_o^2},$$

c_L being a numerical factor. Thus the relative residual interaction spreads the one-body state, $u^c_{n_o}$, through a width, W_o. Since in typical heavy nuclei, the separations, $|\epsilon^c_n - \epsilon^c_{n'}|$, are greater than fifteen MEV and reasonable values for W_o are less than ten MEV, it would seem reasonable that the parent nucleus wave function should contain appreciably only the one-body wave function, $u^c_{n_o}$, and its nearest neighbours. Hence, Eqs. (2.42) and (2.43) should be a moderately good approximation.

The statistical factors, $|C_{n_o c}|^2$, are reasonably interpreted as measuring the probability that the resonant state can be represented by the appropriate decay products. The extent to which the independent-particle model correctly accounts for these correlations will be shown to provide a a test of its validity in the nuclear surface.

CHAPTER 3 EXPERIMENTAL REDUCED WIDTHS

We have contended in the Introduction that the calculations upon alpha-particle decay rates performed by previous authors have, essentially, used the equivalent square-edge nucleus model of Vogt. They have customarily written the decay constant as a product of two factors: a) a nuclear reduced width, which depends only upon the internal aspects of the nucleus and which is interpreted as measuring the frequency at which alpha-particles appear at the nuclear surface; b) a penetrability, which depends only upon the potential barrier and which is interpreted as measuring the ease with which an alpha-particle can penetrate the barrier and appear on the outside. The reduced widths have generally been calculated using square-edge nuclei, while the barrier has generally been rounded-off with the nuclear potential of Igo (1959). Hence, the anomalous reflection of the square-edge nucleus has implicitly been removed; in fact, this corresponds to a calculation with the equivalent square-edge model. In the present section, we will check that previous J.W.K.B. estimates of the penetrabilities are reasonable; in the language of Vogt, this is equivalent to checking that the reflection factors have been calculated accurately. We have also included the penetrability estimates for the unmodified Coulomb barrier. For completeness, we have checked the reduced derivative widths which have been used by some previous authors.

The nuclear reduced width, $|\gamma_c|^2$, is defined in terms of

the probability amplitude,

$$(3.1)\quad \gamma_c = \sqrt{\frac{\hbar^2}{2\mu R_0}} \int_{\mathcal{S}_c} \Psi_0 \, \psi_c \, d\mathcal{S}_c \ .$$

In the channels of alpha-decay, the channel wave functions are of the form,

$$(3.2)\quad \psi_c = \frac{1}{R_0} \chi(\underline{\xi}, \underline{s}_\alpha) \sum_{m_j, M_L} \langle jLm_j M_L | JM \rangle \psi_{jm_j}(\underline{x}_\sigma, \underline{s}_\sigma) Y_L^{M_L}(\Omega),$$

where the single bound-state of the alpha-particle, which has zero angular momentum, has been denoted by $\chi(\underline{\xi}, \underline{s}_\alpha)$ and where the bound states of the daughter functions, $\psi^{\gamma_\sigma}_{j_\sigma m_\sigma}(\underline{x}_\sigma, \underline{s}_\sigma)$, have been denoted by $\psi^{\gamma}_{jm}(\underline{x}_\sigma, \underline{s}_\sigma)$.

It follows from Eq. (2.20) that,

$$(3.3)\quad \gamma_c = \sqrt{\frac{\hbar^2 R_0}{2}} \int_{\Omega, \underline{\xi}, \underline{x}_\sigma, \underline{s}} \Psi_0^* \chi \sum_{m_j, M_L} \langle jLm_j M_L | JM \rangle \psi^{\gamma}_{jm_j} \cdots$$
$$\cdots Y_L^{M_L} \, d\Omega \, d\underline{\xi} \, d\underline{x}_\sigma \, d\underline{s},$$

whence,

$$(3.4)\quad |\gamma_c|^2 = \sum_{n,n'} C^*_{nc} C_{n'c} \gamma^{c*}_n \gamma^c_{n'} \ .$$

It was noted in Chapter 2 that all the coefficients, C_{nc}, may be neglected except $C_{n_0 c}$. Then,

$$(3.5)\quad |C_{n_0 c}|^2 \doteq \frac{|\gamma_c|^2}{|\gamma^c_{n_0}|^2} \ ,$$

and, from Eqs. (2.35) and (2.43),

$$(3.6)\quad \lambda = \sum_c \frac{2 P_c(\epsilon^c_{n_0}, R_0)}{\hbar} |\gamma_c|^2 \ .$$

The reduced derivative width has also been used by some authors, in particular, by Mang (1960). Thomas (1954) has defined the reduced derivative width as,

$$(3.7)\quad |\delta_c|^2 = S_c^2 |\gamma_c|^2 \ ,$$

where S_c is the shift function of Eq. (2.31).

3 - 1: THE REACTION $Po^{212} \longrightarrow Pb^{208} + \alpha$

In the subsequent discussion, only the particularly simple

decay from the ground state of Po^{212} to the ground state of Pb^{208} plus an alpha-particle has been considered. Since the parent nucleus and both of the decay products have spin zero, it is seen that the orbital angular momentum of the alpha-particle relative to the Pb^{208} nucleus must be zero. From Eq. (3.6), the decay constant is then simply,

$$(3.8)\quad \lambda = \frac{2 P_o |\gamma_o|^2}{\hbar} ,$$

where the subscript refers to the relative angular momentum of the channel.

The radial Schroedinger Equation, Eq. (2.14), then becomes,

$$(3.9)\quad -\frac{h^2}{2\mu}\frac{d^2u}{dR^2} + (V_c(R) + V_N(R))\, u = \epsilon_o\, u,$$

where we have neglected the imaginary part of the optical model potential and where we have set the relative orbital angular momentum equal to zero. Here $V_c(R)$ is the electrostatic potential as calculated from the Pb^{208} charge distribution; $V_N(R)$ is the nuclear one-body potential; ϵ_o is the relative energy of the decay fragments. Rasmussen (1959) has stated a value of 8.81 MEV for the decay energy in the laboratory frame yielding a relative decay energy of 8.98 MEV.

In the present calculation, the electrostatic potential has been taken as the Coulomb potential and the nuclear potential as that derived by Igo (1959) from the elastic scattering data:

$$(3.10)\quad V_N(R) = -1100\ \mathrm{EXP}\left(\frac{1.17A^{1/3} - R}{0.574}\right)\ \text{MEV}.$$

$$(\ |V_N(R)| \leq 10\ \text{MEV})$$

The nuclear potential is somewhat uncertain. Firstly, it has been derived at higher energies ($\sim$40 MEV) and it is

probably energy dependent. Secondly, it will be extended inward a little beyond the range of validity determined from the 40 MEV scattering experiments. Thirdly, only the real part of the optical model potential has been used; the scattering data can, in fact, only be fitted with a full optical model potential. It is the imaginary term in the optical model which brings in the many-body aspects of the problem in a phenomenological way; its neglect in the penetrability is justified if the imaginary potential is ascribed to the nuclear interior.

3 - 2: COMPARISONS WITH J.W.K.B. AND SQUARE-WELL ESTIMATES

The penetrability and shift function have been calculated from Eq. (2.31) using Eqs. (3.9) and (3.10). In heavy nuclei, $\overline{G}_0$ is much greater than $\overline{F}_0$ at the nuclear surface so that Eq. (2.31) essentially reduces to,

$$(3.11)\quad P_0(\epsilon_0,R_0) = \frac{kR_0}{\overline{G}_0(R_0)^2}\ ;\ S_0(\epsilon_0,R_0) = R\left.\frac{\frac{d\overline{G}_0(R)}{dR}}{\overline{G}_0(R)}\right|_{R=R_0}\ .$$

$$\left(\ k = \sqrt{\frac{2\nu\epsilon_0}{\hbar}}\ \right)$$

We need therefore only evaluate the irregular function.

The numerical calculation of the shift function and the penetrability has been performed by evaluating the Coulomb functions at 24 fermis with an Airy function expansion and then integrating the irregular solution of Eq. (3.9) backwards to the nuclear surface. This calculation was performed by employing the Runga-Kutta method of order four with the use of the U.B.C. IBM 7040 computer.

In Figure 1, the potentials defined in Eq. (3.9) have

been plotted.

The reduced width and the reduced derivative width have been calculated from Eq. (3.8) and (3.7), respectively; the results of the calculations are tabulated in Table 1.

TABLE 1
EXPERIMENTAL REDUCED WIDTHS

R_o (fermis)	S_o	P_o	γ_o^2 (e.v.)	δ_o^2 (k.e.v.)
10.5	-15.4	3.02×10^{-11}	24	5.9
10.0	-14.1	6.76×10^{-12}	111	22.1
9.5	-11.2	1.72×10^{-12}	436	55.2
9.0	- 4.0	6.71×10^{-13}	1119	17.8

The lifetime of Po^{212} has been taken as 3.04×10^{-7} sec. (Rasmussen (1959)).

The square-well approximation of the penetrability and the shift function are given by,

$$(3.12)\quad P_o(\epsilon_o,R_o) = \frac{kR_o}{G_o(R_o)^2} \quad ; \quad S_o(\epsilon_o,R_o) = R\left.\frac{\frac{dG_o(R)}{dR}}{G_o(R)}\right|_{R=R_o};$$

where G_o is the irregular Coulomb function.

The J.W.K.B. estimate is given by,

$$(3.13)\quad P_o(\epsilon_o,R_o) = qR_o \,\mathrm{EXP}\left(-2\int_{R_o}^{r_o} q(R')dR'\right);$$

$$S_o(\epsilon_o,R_o) = -R_o q(R_o);$$

where R_o is the nuclear radius, r_o is the outer classical turning point, and where

$$q(R) = \frac{\sqrt{2\mu(V_C(R) + V_N(R) - \epsilon_o)}}{\hbar}.$$

In Figure 2, the penetrability, shift function, reduced width, and reduced derivative width have been plotted as

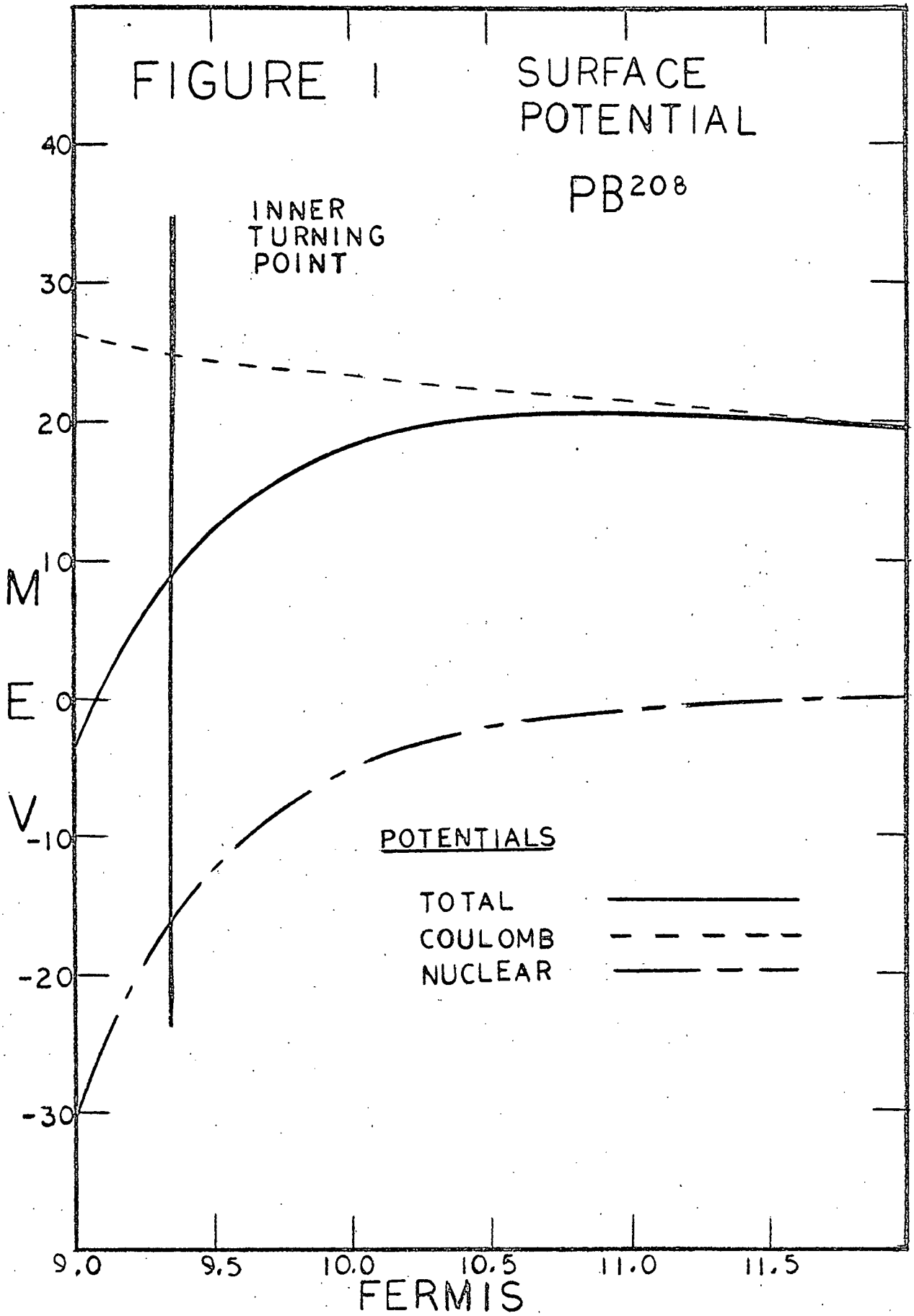
FIGURE 1
SURFACE POTENTIAL
PB208
INNER TURNING POINT
40
30
20
10
0
-10
-20
-30
MEV
POTENTIALS
TOTAL
COULOMB
NUCLEAR
9.0
9.5
10.0
10.5
11.0
11.5
FERMIS

FIGURE 2

PB^{208} PARAMETERS

ACTUAL SQUARE ——

ACTUAL J.W.K.B. – – –

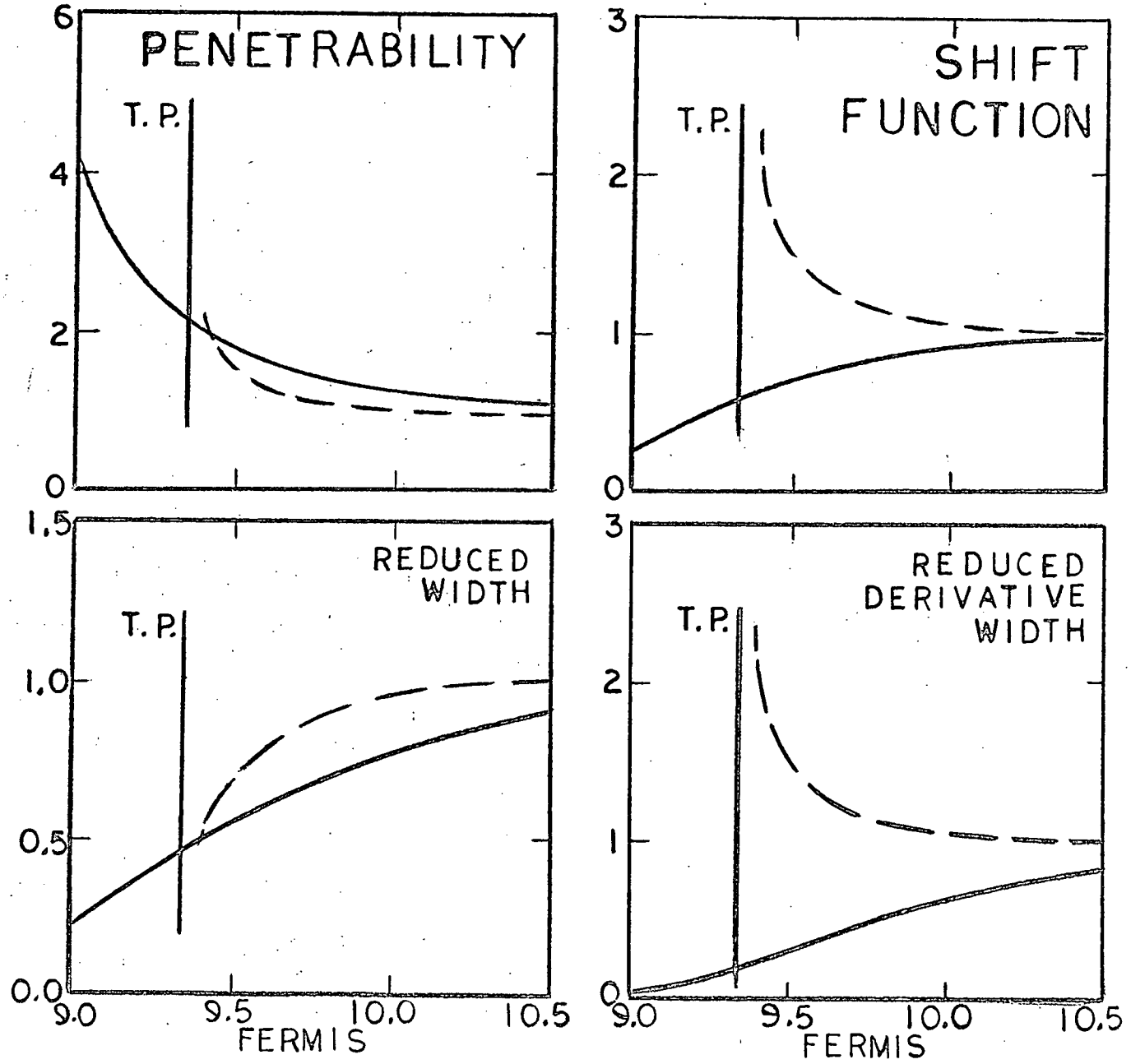

calculated by each of the above methods.

It would seem from Figure 2 that previous estimates of the empirical reduced widths using the J.W.K.B. approximation have not incurred serious error; in fact, the J.W.K.B. approximation is seen to be quite good to within a tenth of a fermi of the classical inner turning point. It is also seen that the error incurred in using the unmodified Coulomb barrier is less than an order of magnitude outside of the classical inner turning point.

Bencze and Sandelescu (1966) have recently investigated the validity of the J.W.K.B. estimate of the penetrability in the reaction $Pu^{238} \longrightarrow U^{234} + \alpha$. They find that the J.W.K.B. estimate is low by a factor of from two to five near the inner turning point, in agreement with the results presented in this chapter. In fact, they claim a much deeper one-body potential than is customarily believed ($\sim$ 231 MEV) and, in this manner, obtain a further increase in the penetrabilities. In Chapter 4, we show that, if the nuclear surface is treated in a direct manner, it is not necessary to resort to such extreme well depths to obtain a reasonable agreement with the empirical decay rates.

CHAPTER 4 INDEPENDENT-PARTICLE MODEL DECAY RATES OF Po^{212}

In the present chapter, we will examine the effect of the diffuse nuclear edge upon the calculated alpha-particle decay rates of heavy nuclei. In particular, we will re-examine the square-well calculation of the alpha-particle decay rate of Po^{212} performed by Harada (1961). With the inclusion of configuration mixing, Harada has obtained reasonable agreement with the empirical decay rates, but has had to resort to larger radii than those believed to be typical of a heavy nucleus. It is our contention that his calculation corresponds to a calculation with the equivalent square-edge nucleus model of Vogt; in fact, we will show that the radius involved in this model is much larger than that of the conventional diffuse-edge nucleus to which it corresponds. We will also repeat the calculation of Harada, introducing the diffuse-edge into the calculation in a direct manner.

The effect of the shape and surface of the nucleus upon the decay rates is, primarily, a one-body effect. By this we mean that in Eq. (2.37),

$$\lambda = \sum_c \lambda_c^{o.b.} S_c \,, \tag{2.37}$$

the one-body decay constants, $\lambda_c^{o.b.}$, are quite sensitive to the size and to the nature of the surface of the nucleus whereas the spectroscopic factors, S_c, are rather insensitive to these characteristics. It is our contention that previous calculations have calculated the spectroscopic factors (and, hence, the many-body effects) correctly, but have misinterpreted the radius involved in the calculation of the one-body

decay constant.

It has been customary in previous calculations to calculate the alpha-particle decay rates from Eq. (3.6):

$$(3.6)\quad \lambda = \sum_c \frac{2P_c(\epsilon^c_{n_o}, R_o)}{\hbar} |\gamma_c|^2 .$$

The penetrability has, generally, been calculated for a diffuse-edge barrier, as has been discussed in Chapter 3. On the other hand, the nuclear reduced width has, generally, been calculated by using the resonant one-body wave function of a square-edge well in the following sense: one sets the amplitude of that mode of the nuclear wave function which describes the relative motion of the decay products equal to the amplitude of the resonant one-body wave function at the nuclear radius. It is in the sense of the latter procedure that the nucleus is taken to be square. We have noted in Chapter 3 that these procedures for calculating the decay rates correspond to a calculation with the equivalent square-edge nucleus of Vogt (1962).

It is of heuristic value to consider the freedom with which an alpha-particle can move within the nucleus. To see how far an alpha-particle can travel in the nuclear volume before being absorbed, consider a square-well potential having typical real and imaginary parts, V_o and W_o, such that

$$V_o >> W_o, \epsilon_o .$$

Assuming the Coulomb effects to be incorporated in V_o, the regular solution of Eq. (3.9) is of the form,

$$U(R) = \sin KR,$$

where,

$$K \sim k\sqrt{\frac{V_o}{\epsilon_o}} + i\frac{kW_o}{2\sqrt{V_o\epsilon_o}} \quad . \quad \left(k = \frac{\sqrt{2\mu\epsilon_o}}{\hbar} \sim 1.3\right)$$

For a typical heavy nucleus, V_o may be taken to be about 100 MEV and W_o to be from 5 MEV to 10 MEV. The mean free path of an alpha-particle within the nuclear volume,

$$(4.1) \quad l_N \sim \frac{\sqrt{V_o\epsilon_o}}{kW_o} \quad ,$$

then ranges from about five to about two fermis (respectively). There is some evidence that the imaginary potential is large only in the surface region, so that the alpha-particle might have even greater freedom within the nuclear volume; in general, W is then larger in the surface region so that here the alpha-particle has less freedom. Thus, to the extent that the one-body model is valid, the alpha-particle moves rather freely within the nucleus except in the vicinity of the nuclear surface.

It can easily be shown from the J.W.K.B. approximation that the mean free path of an alpha-particle in the barrier region is about,

$$(4.2) \quad l_b \sim \frac{1}{2k\sqrt{\frac{V}{\epsilon_o} - 1}} \quad ,$$

where V is the height of the barrier. If we attribute the many-body aspects of the problem to the nuclear interior, we may take the imaginary potential (which accounts for the many-body aspects of the problem) as vanishing outside the nuclear radius. This is the assumption made in Chapter 3, where we have attributed all the penetration effects of the barrier to the penetrabilities, and is probably extreme. With this assumption, it is seen from Figure 1 and Eq. (4.2) that the

mean free path in the barrier and near the surface for a square-edge well is considerably less than that for the diffuse-edge well. It is in this sense that we expect a diffuse-edge well to behave like a square-edge well of larger radius.

In the discussion to follow, this effect is developed from the following point of view. The effect of the diffuse-edge on the one-body resonant wave functions is examined and it is found that the diffuse-edge enhances the resonant wave function at and beyond the nuclear radius. Hence, the one-body reduced widths are enhanced in a similar manner. From Eq. (2.40), one would expect to observe this enhancement in the elastic scattering cross-sections (the width of the elastic scattering cross-section is proportional to the decay constant). We have demonstrated this in a direct manner by calculating the differential elastic scattering cross-section of Pb^{208} at 90^0_{CM} . We have included the many-body effects by repeating the independent-particle model calculation of the decay constant of Po^{212} performed by Harada (1961) with the diffuse-edge of the nucleus now being taken into account in a direct manner.

4 - 1: ONE-BODY REDUCED WIDTHS AND EXPERIMENTAL SPECTROSCOPIC FACTORS

In the present section, we will examine the effects of diffuse-edge of the nucleus upon the one-body reduced widths. We also provide an estimate of the correction in the experimental spectroscopic factors due to the diffuse-edge.

The reduced mass in Eq. (3.9) has the value 5.9031×10^{-24} grams.

The electrostatic potential, $V_C(R)$, has been calculated from the Pb^{208} charge distribution of Hill and Ford (1955):

$$(4.3)\qquad \rho(R) = \begin{cases} 1 - \frac{1}{2}\,\mathrm{EXP}(R/6.7 - 10) & \text{if } R \leq 6.7 \text{ f.} \\ \frac{1}{2}\,\mathrm{EXP}(10 - R/6.7) & \text{if } R > 6.7 \text{ f.} \end{cases}$$

Then,

$$(4.4)\qquad V_C(R) = 82 \times 2 \times e^2 \times \left[\frac{1}{R} \int_0^R \rho(R')R'^2 dR' + \cdots \right.$$
$$\left. \cdots + \int_R^{R_0} \rho(R')R'dR' \right] \times \left[\int_0^{R_0} \rho(R')R'^2 dR' \right]^{-1}.$$

The nuclear potentials, $V_N(R)$, have been chosen to be of the Saxon-Woods form,

$$(4.5)\qquad V_N(R) = V_0 \times \left[1 + \mathrm{EXP}\left((R - r_0)/a \right) \right]^{-1}.$$

In Figure 3, the potentials have been plotted corresonding to a nuclear Saxon-Woods shape of thickness (a) 0.5 fermis, radius (r_0) 9.0 fermis, and depth (V_0) 105 MEV; we have also plotted a square-well of the same radius and of a similar depth. The depths of the wells were chosen so that the regular solutions of Eq. (3.9) were resonant and had the same number of nodes; these resonant wave functions have been plotted in Figure 4.

The analysis of decay rates and scattering cross-sections assigns all of the effects of the interior of the nucleus to the reducd widths, these being evaluated in the nuclear surface. It is exactly in this sense that the diffuse-edge well can be replaced by a square-edge well of greater radius. If the diffuse-edge well is replaced by that square-edge well having a radius such that their reduced widths are equal, the wells are indistinguishable within the nuclear volume; the difference in the reflection of the wells outside of the

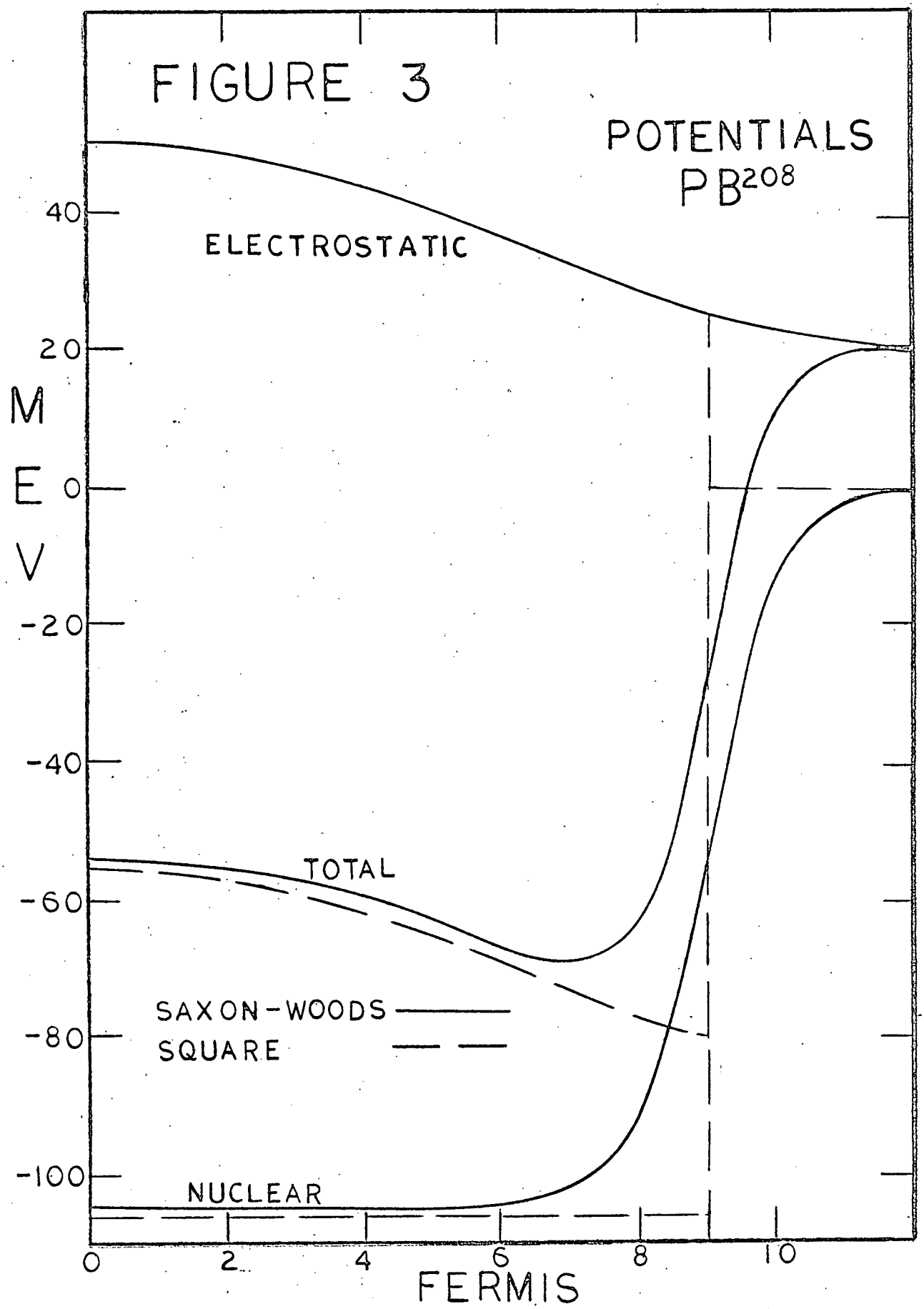
FIGURE 3
POTENTIALS
PB208
ELECTROSTATIC
TOTAL
SAXON-WOODS
SQUARE
NUCLEAR
MEV
40
20
0
-20
-40
-60
-80
-100
0
2
4
6
8
10
FERMIS

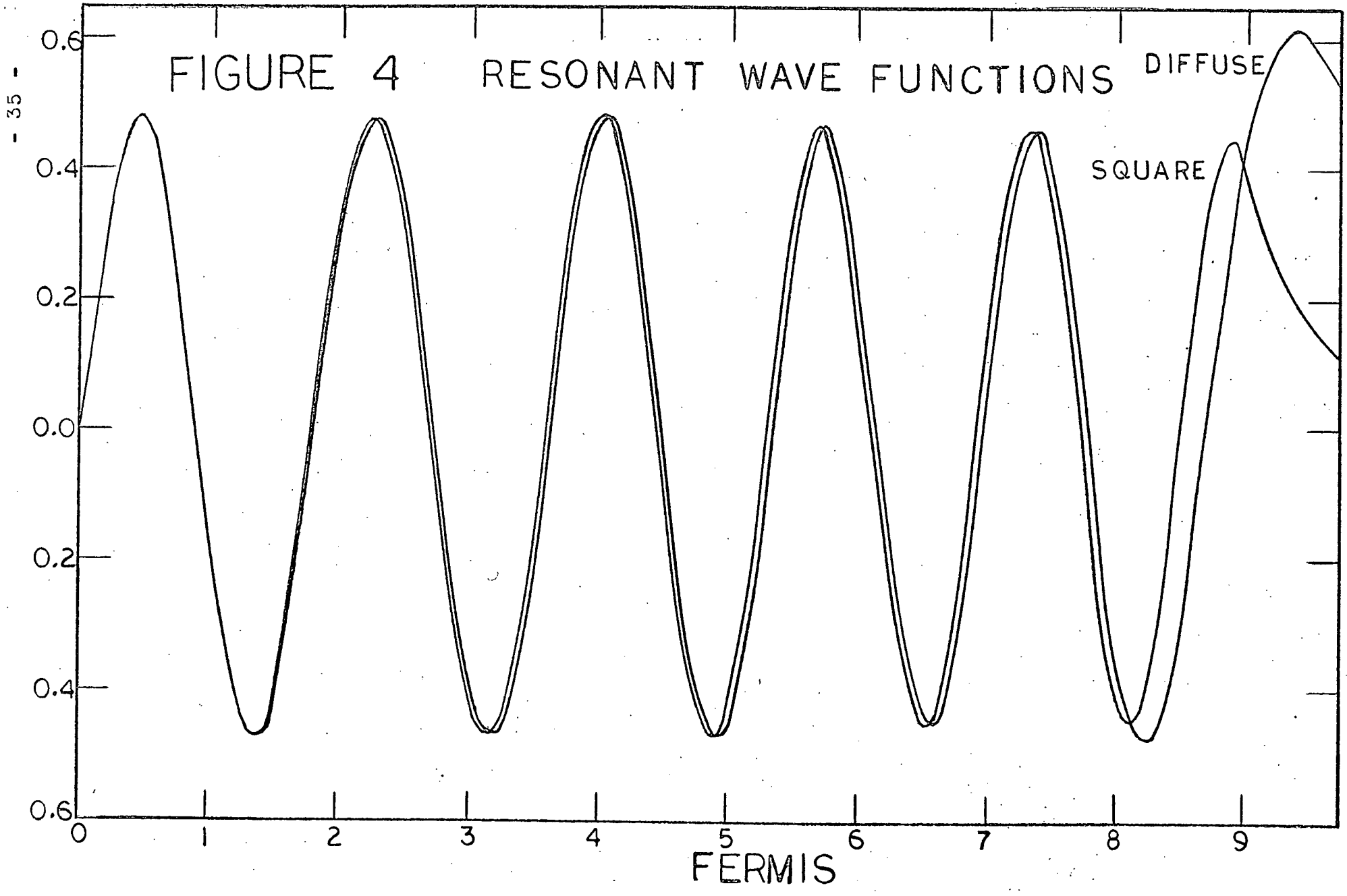
FIGURE 4 RESONANT WAVE FUNCTIONS
DIFFUSE
SQUARE
0.6
0.4
0.2
0.0
0.2
0.4
0.6
0
1
2
3
4
5
6
7
8
9
FERMIS

nuclear volume is accounted for by a typically small reflection factor. In fact, this is essentially the equivalent square-edge nucleus model of Vogt (1962).

It is seen from Figure 4 that the radius of this "equivalent square-well" should be significantly larger than the radius of the diffuse-edge well. This is the basis of our contention that a diffuse-edge well should behave like a larger square-edge well in the analysis of decay rates. To exhibit this clearly, we will calculate the one-body reduced widths with a diffuse-edge well and compare them with the square-edge well estimate of Harada (1961).

A single nucleon in a heavy nucleus moves in a potential having a depth of about 50 MEV. It would, therefore, seem that reasonable depths for the potential well should lie between 50 MEV and 200 MEV, values of 100-150 MEV currently being fashionable. It is also seen from Eq. (3.10) that the Igo potential is known inwards only to about 9.7 fermis so that the shape of the well edge may be chosen rather arbitrarily within this radius. It, therefore, seemed reasonable to choose the potentials of the type of Eq. (4.5) in the following manner.

The thickness of the surface, a, was chosen to have the values tabulated in Table 2. The depth, V_0, and the radius, R_0, were then varied so that the potential was simultaneously equal to the Igo potential at 10 fermis and so that the regular solution of Eq. (3.9) was asymptotic to the irregular Coulomb function --- the condition for resonance. (There is

only one such potential for a given number of nodes.) By the discussion of Chapter 2, one of these potentials should be a good representation of the actual potential. Exactly which one is the actual potential cannot be decided until some further criterion is established for deciding the well depths more precisely. Neither fundamental nuclear theory not the analysis of alpha-particle scattering data defines the well depth very clearly within the range 50 MEV to 150 MEV.

Examples of the resulting potentials are summarized in Table 2. The behaviour of the resonant wave functions as a function of the well depth has been illustrated in Figure 5 and their behaviour as a function of surface thickness in Figure 6.

TABLE 2
ONE-BODY POTENTIALS

POTENTIAL V_N	NODES n_o	THICKNESS a (fermis)	DEPTH V_o (MEV)	RADIUS r_o (fermis)
A	4	0.5	- 49.1	8.94
B	6	0.5	- 64.5	8.79
C	8	0.5	- 86.3	8.63
D	10	0.5	-114.5	8.48
E	12	0.5	-149.6	8.34
F	10	0.3	-103.4	9.12
G	10	0.7	-128.9	7.79

The one-body reduced widths have been calculated from the resonant wave functions (Eq. (2.33)) and have been used

to calculate the experimental spectroscopic factors (Eq. (3.5) and Table 1).

TABLE 3
EXPERIMENTAL SPECTROSCOPIC FACTORS

POTENTIAL	EVALUATED AT 9.0 f.			EVALUATED AT 10.0 f.		
	$\gamma^2_{n_o}$ (kev)	γ^2_{exp} (kev)	$C^2_{n_o}$	$\gamma^2_{n_o}$ (kev)	γ^2_{exp} (kev)	$C^2_{n_o}$
A	105	1.12	1.07×10^{-2}	11.5	0.111	0.98×10^{-2}
B	150	1.12	0.75 "	16.9	0.111	0.66 "
C	188	1.12	0.59	21.8	0.111	0.51
D	223	1.12	0.50	26.3	0.111	0.42
E	256	1.12	0.44	30.5	0.111	0.36
F	101	1.12	1.11	42.4	0.111	0.26
G	170	1.12	0.65	15.5	0.111	0.71

If the potentials chosen in evaluating the experimental reduced widths and the one-body reduced widths had been the same, the experimental spectroscopic factors would be independent of the radius. The radial dependence has been included to indicate the effect of the nature of the surface chosen and, for reasonable surface thicknesses of 0.5 - 0.7 fermis, this is seen to be slight.

Harada, using a square-edge well of radius 10 fermis, has obtained a value of 0.143 for the experimental reduced width and a value of 0.08×10^{-2} for the experimental spectroscopic factor. It would appear from Table 3 that the spectroscopic factor might be about an order of magnitude larger than this value.

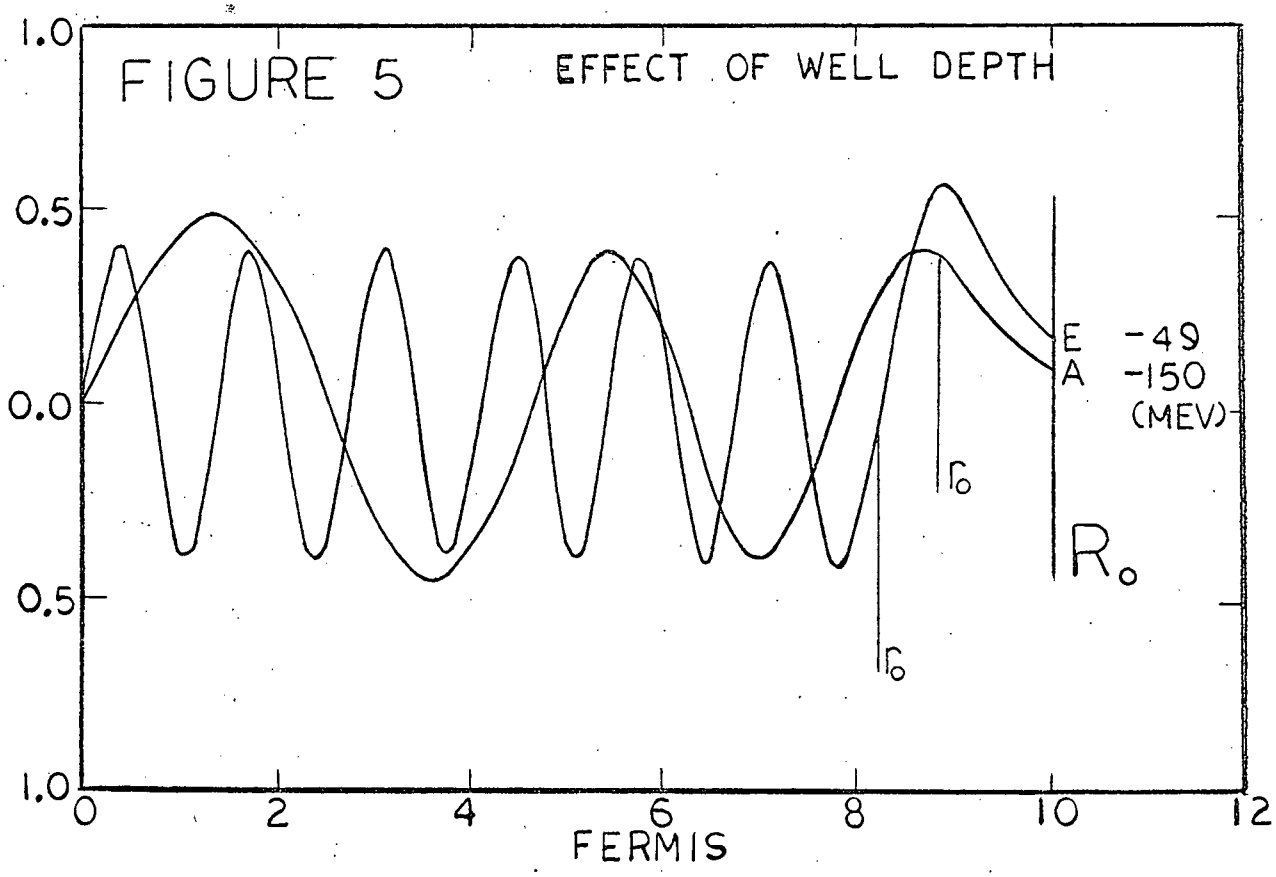
FIGURE 5
EFFECT OF WELL DEPTH
1.0
0.5
0.0
0.5
1.0
0
2
4
6
8
10
12
FERMIS
E -49
A -150
(MEV)
r_o
r_o
R_o

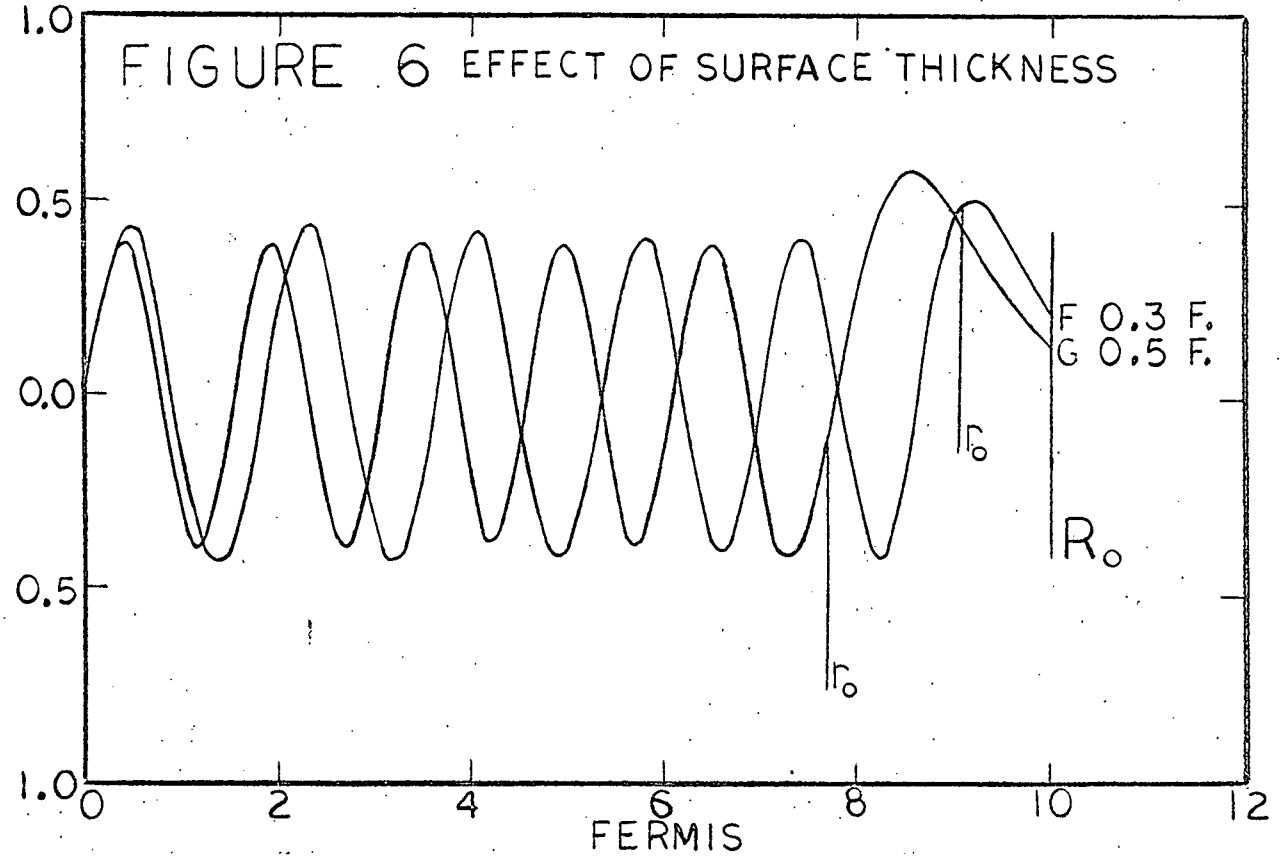
FIGURE 6 EFFECT OF SURFACE THICKNESS
1.0
0.5
0.0
0.5
1.0
0
2
4
6
8
10
12
FERMIS
F 0.3 F.
G 0.5 F.
r_o
r_o
R_o

4 - 2: ONE-BODY DIFFERENTIAL ELASTIC SCATTERING CROSS-SECTION OF Pb^{208} FOR AN ALPHA-PARTICLE AT 90^0_{CM}

One of the most direct ways in which to illustrate the effects of the diffuse-edge on the decay rates is to calculate its effect on the one-body elastic scattering cross-sections. (As has previously been noted, the one-body width is proportional to the one-body decay constant.) In this section, the one-body differential elastic scattering cross-section for the scattering of an alpha-particle from the ground state of Pb^{208} will be calculated by direct and well-known procedures. What one does is to study the behaviour of the logarithmic derivative of the wave function about the resonance; the one-body width can then be calculated in a straightforward manner. The procedure for calculating the cross-sections by these techniques is discussed in Appendix C.

It is worth noting that the calculation of the logarithmic derivative is very tedious due to the very small widths involved; in fact, the calculations performed in this thesis required seventeen place accuracy in the potentials and required many hours of computer time on the IBM 7040 computer used in these calculations. For this reason, such direct calculations have previously been avoided by other authors.

The $Pb^{208}(\alpha,\alpha)Pb^{208}$ differential elastic scattering cross-section at 90^0_{CM} has been plotted in Figure 7, both for a square-well and for a diffuse-edge well of the same radius. It is seen that the diffuse-edge enhances the elastic scattering cross-section (and, hence, the one-body decay

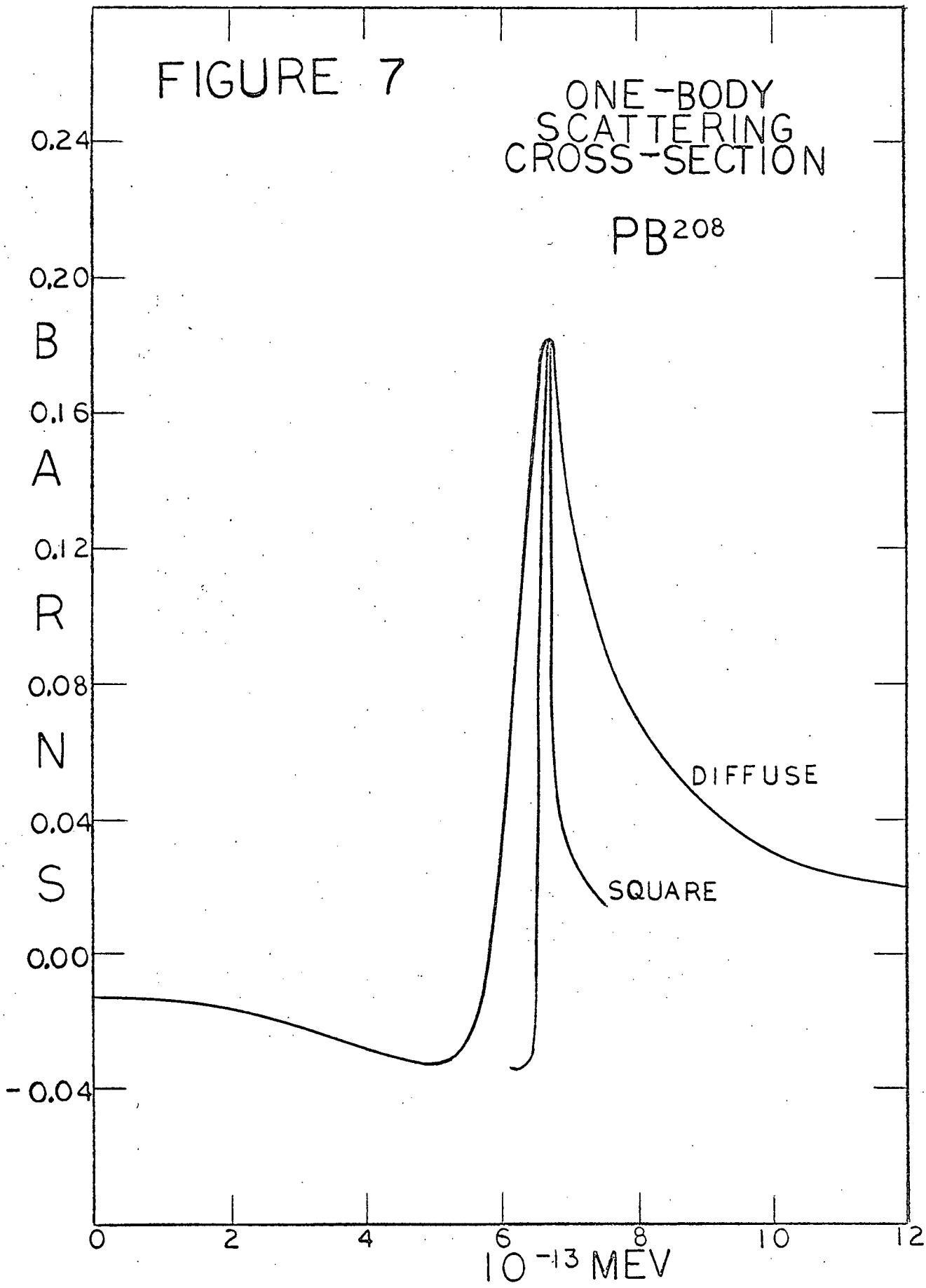
FIGURE 7
ONE-BODY
SCATTERING
CROSS-SECTION
PB208
0.24
0.20
B
0.16
A
0.12
R
0.08
N
0.04
S
0.00
-0.04
DIFFUSE
SQUARE
0
2
4
6
8
10
12
10-13 MEV

constant) by about an order of magnitude.

The diffuse-edge well has here been taken to be of the Saxon-Woods type, Eq. (4.5), with the parameters,

$$V_o = -48.9 \text{ MEV}; \quad r_o = 9.0 \text{ f.}; \quad a = 0.5 \text{ f.};$$

the parameters of the square-well are taken to be,

$$V_s = -47.8 \text{ MEV}; \quad r_s = 9.0 \text{ f.}$$

The depths of the wells have been chosen so that the wave functions are resonant at 8.9795 MEV and have the same number of nodes.

The cross-sections have been plotted by studying the behaviour of the logarithmic derivative of the wave functions at 24.0 fermis.

A width of 1.37×10^{-13} MEV was found for the diffuse-edge well and a width of 1.94 MEV for the square-edge well; hence, the enhancement in the cross-section (or decay constant) due to the diffuse-edge is a factor of 7.1.

4 - 3: HARADA'S FORMULA FOR INDEPENDENT-PARTICLE MODEL REDUCED WIDTHS

A convenient technique for evaluating independent-particle model reduced widths has been developed by Harada (1961). We provide here only an outline of his result for the simple case of Po^{212}; a more complete discussion is given in Appendix A.

It will be assumed that the zeroth order approximation of Eq. (2.25) can be described by the ground state configuration of the independent-particle model. Employing the partial antisymmetrization scheme of Chapter 2, and neglecting core excitations, the parent nucleus wave function can be

written in the form,

$$(4.6)\quad \Psi_0(12\ldots A) = \phi_\alpha(1234)\,\psi^\tau_{00}(56\ldots A)\ ,$$

where ψ^τ_{00} is the wave function of the doubly magic Pb^{208} core. (The notation is that of Chapter 2.) From Eq. (3.3), and noting that the parent nucleus, daughter nucleus, and alpha-particle have spin zero,

$$(4.7)\quad \gamma_c = \sqrt{\frac{h^2R_0}{\mu}} \int_{\Omega,\underline{\xi},\underline{s}_\alpha} \phi^*(1234)\,\chi(1234)\,Y^0_0(\Omega)\,d\Omega\,d\underline{\xi}\,d\underline{s}_\alpha\ .$$

Harada has chosen the alpha-particle wave function to be of the Gaussian type:

$$(4.8)\quad \chi(1234) = \left(\frac{\beta^{3/2}}{(\frac{1}{2}!)}\right)^{3/2} \mathrm{EXP}\left(-\frac{\beta}{2}\left(\frac{\xi_1^2}{2} + \frac{\xi_2^2}{2} + \xi_3^2\right)\right)$$
$$\cdots\ (4\pi)^{-3/2}\,\chi^0_0(12)\,\chi^0_0(34)\ ,$$

where χ^0_0 denotes the spin singlet function. Here, $\underline{\xi}_i$ has been written in terms of its radial and angular components, ξ_i and Ω_i, respectively.# Harada chooses the parameter β so that the r.m.s. radius of the charge density is equal to the measured value (1.6 fermis); he finds a value of 0.44 fermis^{-2} for β.

In Appendix A, it is shown that Eq. (4.7) can be written in the form,

$$(4.9)\quad \gamma_c = \sqrt{4\pi}\sqrt{\frac{h^2R_0}{2\mu}}\ \left[T(00;j_1j_1)\ T(00;j_3j_3)\right]$$
$$\cdots\left[\int_{\Omega,\xi_1,\xi_2,\xi_3,\underline{s}_\alpha} \sum_{\substack{n_1,n_2,\\ n_3}} \langle N_1 0 n_1 0;0|\upsilon_1 l_1 \upsilon_1 l_1;0\rangle\right.$$
$$\cdots\langle N_2 0 n_2 0;0|\upsilon_3 l_3 \upsilon_3 l_3;0\rangle\langle N 0 n_3 0;0|\,N_1 0 N_2 0;0\rangle$$
$$\left.\cdots\psi_{n_1 0}(\xi_1)\psi_{n_2 0}(\xi_2)\psi_{n_3 0}(\xi_3)\psi_{N0}(R_0)\right]$$
$$\cdots\ \left[\chi^8(12)\,\chi^0_0(34)\right]\,d\Omega\,\xi_1^2 d\xi_1 \xi_2^2 d\xi_2 \xi_3^2 d\xi_3 d\underline{s}_\alpha\ .$$

Here it has been assumed that the one-nucleon wave functions

The definition of ξ_i differs from Harada's. (c.f. Appendix A)

for the two protons (neutrons) in the unfilled shell are described by the quantum numbers $(\nu_1 l_1 j_1 m_1)$ ($(\nu_3 l_3 j_3 m_3)$), where ν_1 (ν_3), l_1 (l_3), j_1 (j_3), and m_1 (m_3) denote the principal quantum number, the orbital angular momentum, the total angular momentum, and the magnetic quantum numbers of the one-proton (one-neutron) orbitals. In Eq. (4.9), the first bracketed term contains the T coefficients of Rose (1957) for transforming the j - j coupling scheme to an L - S coupling scheme; the second bracketed term expands the wave function in terms of the relative co-ordinates; the final bracketed term contains the spin functions. A statistical constant and a double parentage coefficient, both of which are unity, have been omitted from the discussion. $\psi_{n_i 0}$ (i = 1,2,3) and ψ_{N0} are one-nucleon orbitals of zero angular momenta with principal quantum numbers n_i (i = 1,2,3) and N, respectively. The coefficients appearing in the summation of the second bracketed term are the Talmi coefficients (Talmi (1952)); a formula for the Talmi coefficients incurred in the transformation of harmonic oscillator wave functions is derived in Appendix B.

The radial harmonic oscillator wave function is of the form,

$$(4.10)\quad \psi_{nl}(r) = \sqrt{\frac{2n!\,b^{3/2}}{(n+l+\frac{1}{2})!}}\; L_n^{l+\frac{1}{2}}(br^2)\; (\sqrt{b}r)^l\; e^{-\frac{1}{2}br^2},$$

where,

$$L_n^{l+\frac{1}{2}}(br^2) = \sum_{h=0}^{n} \binom{n+l+\frac{1}{2}}{n-h} \frac{(-1)^h}{h!}\, (br^2)^h,$$

b being the harmonic oscillator size parameter. It will be convenient to write Eq. (4.7) in the form,

$$(4.11)\quad \gamma_c = \sqrt{\frac{h^2 R_o}{2\mu}} \sum_N \mathcal{O}_N(R_o),$$

and to assume that the one-nucleon wave functions of the independent-particle model and the functions $\psi_{n_i o}$ (i = 1,2,3) and ψ_{N0} can be approximated by harmonic oscillator wave functions. The overlap integral,

$$(4.12)\quad (R_o) = \sum_N \mathcal{O}_N(R_o),$$

is found by performing the integrations; the result is,

$$(4.13)\quad \mathcal{O}_N(R_o) = T(00;j_1 j_1)\, T(00;j_3 j_3) \sum_{n_1 n_2} \langle N 0 n_3 0;0 | N_1 0 N_2 0;0\rangle$$
$$\cdots \langle N_1 0 n_1 0;0 | \nu_1 l_1 \nu_1 l_1;0\rangle \langle N_2 0 n_2 0;0 | \nu_3 l_3 \nu_3 l_3;0\rangle$$
$$\cdots (\tfrac{1}{2}!)^{-3/2} \left[\frac{(n_1+\frac{1}{2})!(n_2+\frac{1}{2})!(n_3+\frac{1}{2})!}{n_1! n_2! n_3!}\right]^{\frac{1}{2}} \left(\frac{2\sqrt{\beta b}}{\beta + b}\right)^{9/2}$$
$$\cdots \left(\frac{\beta - b}{\beta + b}\right)^{n_1+n_2+n_3} \psi_{N0}(R_o) \quad .$$

The radial functions, ψ_{N0}, define the center-of-mass dependence of the system (1234). If most of the contribution comes from a principal node, N_o, one would expect the principal function, $\psi_{N_o 0}$, to be similar to the resonant solution of Eq. (3.9) having the same number of nodes. Since the only free parameter of the harmonic oscillator wave function is the size parameter, b, its choice must be somewhat arbitrary. Since only the amplitudes enter the determination of the reduced width, it might seem reasonable to choose the amplitude of the principal function at the nuclear radius to be equal to the corresponding amplitude of the one-body wave function as selected from Table 2. Of course, such a solution will, in general, neither yield the correct energy nor satisfy the boundary

condition, Eq. (2.30).

It is not clear that connecting the independent-particle model calculation with the one-body problem in the above manner introduces the surface and the size effects of the one-body problem into the calculation correctly. It is seen from Eq. (3.5) that the spectroscopic factors should be rather insensitive to the surface and the size of the nucleus so that these features should affect only the one-body aspects of the calculation; in fact, in this calculation, the spectroscopic factors are connected to the one-body problem only through the choice of the size parameter. Hence, if the use of the harmonic oscillator one-nucleon functions is reasonable, the criterion for the validity of the above procedure becomes that the spectroscopic factors must not depend sensitively upon the choice of the size parameter.

4 - 4: NUMERICAL INDEPENDENT-PARTICLE MODEL REDUCED WIDTHS

In the present section, we will calculate the independent-particle model reduced width of Po^{212} by the technique of Harada, but employing the one-body resonant wave functions of a diffuse-edge well rather than those of a square-edge well. In his calculation, Harada has assumed a square-edge well of radius ten fermis; with the introduction of configuration mixing in the parent nucleus wave function, he obtains a reasonable value of about one-twentieth the empirical decay constant. A larger radius would produce a larger decay constant but, from Figure 1, it would appear that over ten fermis is too large a nuclear radius. In fact, as will be shown in the sub-

sequent discussion, this large square-edge well corresponds to a smaller diffuse-edge well.

Harada has chosen the size parameter so that the principal function should have an amplitude at the nuclear radius (ten fermis) equal to that of a square-well resonant wave function; the square-well has been chosen so that this wave function has the same number of nodes as the principal function and satisfies the boundary condition, Eq. (2.30), exactly. The only aspect in which the present calculation differs from Harada's is that the size parameter has been chosen so that the amplitude of the principal function is equal to the amplitude of the corresponding resonant function of a diffuse-edge well as selected from Table 2. This procedure is intended to incorporate the properties of the diffuse-edge into the calculated reduced widths in a more direct way. It makes much clearer the role of the potential and the value of the radius of the resonant state.

The contributions to the overlap integral from each node, $\mathcal{O}_N(R_o)$, are given in Table 4. Here, the principal function has been chosen to have ten nodes and the results are tabulated for various nuclear sizes and surface thicknesses. The rates of contribution were found to be rather insensitive to the harmonic oscillator size parameter.

The calculated values of the reduced widths are tabulated in Table 5. A comparison with the experimental values (Table 1) and, hence, of the decay rates, has also been included in the tabulation.

TABLE 4
OVERLAP INTEGRALS

a) Surface Thickness: 0.5 fermis

$(f.^{-3/2})$	R_o = 9.0 f. #b = 0.116 $f.^{-2}$	R_o = 9.5 f. b = 0.095 $f.^{-2}$	R_o = 10.0 f. b = 0.116 $f.^{-2}$
$\mathcal{O}_4$	5.68×10^{-8}	2.73×10^{-7}	1.76×10^{-9}
$\mathcal{O}_5$	4.43×10^{-8}	1.67×10^{-7}	1.83×10^{-9}
$\mathcal{O}_6$	4.89×10^{-7}	1.43×10^{-6}	2.75×10^{-8}
$\mathcal{O}_7$	7.98×10^{-6}	1.75×10^{-5}	6.35×10^{-7}
$\mathcal{O}_8$	6.06×10^{-5}	9.62×10^{-5}	7.18×10^{-6}
$\mathcal{O}_9$	1.31×10^{-4}	1.39×10^{-4}	2.46×10^{-5}
$\mathcal{O}_{10}$	9.61×10^{-5}	5.41×10^{-5}	3.32×10^{-5}
$\mathcal{O}_{11}$	1.59×10^{-5}	1.08×10^{-6}	1.42×10^{-5}

This was the largest possible amplitude and is slightly less than the resonant amplitude.

b) Surface Thickness: 0.7 fermis

$(f.^{-3/2})$	R_o = 9.0 f. b = 0.110 $f.^{-2}$	R_o = 9.5 f. b = 0.092 $f.^{-2}$	R_o = 10.0 f. b = 0.120 $f.^{-2}$
$\mathcal{O}_4$	1.26×10^{-7}	3.93×10^{-7}	9.27×10^{-10}
$\mathcal{O}_5$	8.84×10^{-8}	2.28×10^{-7}	1.01×10^{-9}
$\mathcal{O}_6$	8.75×10^{-7}	1.84×10^{-6}	1.62×10^{-8}
$\mathcal{O}_7$	1.27×10^{-5}	2.10×10^{-5}	3.99×10^{-7}
$\mathcal{O}_8$	8.36×10^{-5}	1.06×10^{-4}	4.82×10^{-6}
$\mathcal{O}_9$	1.51×10^{-4}	1.36×10^{-4}	1.78×10^{-5}
$\mathcal{O}_{10}$	8.52×10^{-5}	4.05×10^{-5}	2.61×10^{-5}
$\mathcal{O}_{11}$	6.81×10^{-6}	4.49×10^{-6}	1.23×10^{-5}

TABLE 5
COMPARISON OF DECAY RATES

Size of Nucleus	R_o (f.)	a (f.)	γ^2_{theor} (ev)	γ^2_{exp} (kev)	$\frac{\lambda_{theor}}{\lambda_{exp}}$
~8.5 f.	9.0	0.5	5.20	1.119	1/220
	9.5	0.5	5.19		
	10.0	0.5	0.36	0.111	1/310
~8.0	9.0	0.7	6.16	1.119	1/180
	9.5	0.7	5.18		
	10.0	0.7	0.22	0.111	1/500
#Harada: ~10.0	10.0	0.0	1.3	0.143	1/110

(Harada (1961))

We have previously noted that the spectroscopic factors should be rather insensitive to the size and the surface of the nucleus. In Table 6, the spectroscopic factors found in the present calculation have been compared with those of Harada.

TABLE 6
CALCULATED SPECTROSCOPIC FACTORS

Size of Nucleus	Surface Thickness	Evaluated at 9.0 f. $C^2_{n_o}$	Evaluated at 10.0 f. $C^2_{n_o}$
~8.5 f.	0.5 f.	2.4×10^{-5}	1.3×10^{-5}
~8.0 f.	0.7 f.	3.6×10^{-5}	1.4×10^{-5}
#Harada: ~10.0 f.	0.0 f.		0.9×10^{-5}

(Harada (1961))

It is seen from Table 5 that, by treating the one-body aspects of the problem with a diffuse-edge well, an agreement with the empirical decay rates can be obtained that is as good as that found by Harada employing an anomalously large radius; in fact, the values suggested for the nuclear sizes in Table 5 are rather modest sizes for heavy nuclei. Harada has found that the introduction of configuration mixing increases the calculated decay rates by a factor of between five and ten. It should be possible to remove much of the remaining discrepancy by choosing a larger, but still reasonable, size for the nucleus.

CHAPTER 5 THE EQUIVALENT SQUARE-EDGE NUCLEUS MODEL

In the present chapter, we will define, for a conventional diffuse-edge nucleus, a square-edge nucleus which, for the purposes of studying decay rates, scattering data, and absorption processes, exhibits many of the properties of the diffuse-edge nucleus to which it corresponds. In fact, the "equivalent square-edge nucleus" which we will define is, essentially, that which has been used by previous authors, in particular Harada (1961), in the calculation of the alpha-particle decay rates of heavy nuclei.

The usefulness of replacing a diffuse-edge nucleus with an "equivalent" square-edge nucleus has been noted previously by Vogt (1962); he has defined and employed the "equivalent square-edge nucleus" in the analysis of the scattering and absorption of neutrons. In particular, he has found that the parameters of this model are insensitive to the incident energy and channel and also to the many-body aspects of the nuclear problem; hence, the equivalent square-edge nucleus is defined in a reasonably unique manner for a given diffuse-edge nucleus. Vogt, Michaud, and Reeves (1965) have found similar results for alpha-particle scattering from light nuclei. The usefulness of the equivalent square-edge nucleus is then two-fold: a) once having determined the parameters of the model, it allows one to exploit the simple analytic properties of square-wells in subsequent calculations; b) it provides a convenient set of parameters for studying the effect of the diffuse nuclear edge on decay rates, scattering cross-sections, and ab-

sorption cross-sections. This is particularly helpful in the study of absorption cross-sections at the low energies of interest to astrophysics where the calculations are otherwise quite tedious.

In the discussion to follow, we will provide the definition of the equivalent square-edge nucleus model and will check the extent to which it applies to alpha-particle scattering and absorption in heavy nuclei.

5 - 1: THE EQUIVALENT SQUARE-EDGE NUCLEUS MODEL

The equivalent square-edge nucleus of a diffuse-edge nucleus is defined in the following manner. The radius and depth of a real square-well potential are chosen so that the following conditions are satisfied: a) it exhibits a resonant wave function in the channel, c, at the resonance energy, ϵ_c, appropriate to the decay, scattering, or absorption problem of interest; b)the resonant wave function of the square-well has the same number of nodes as that of the corresponding resonant function of the diffuse-edge well which describes the average interaction between the incident particle and the target nucleus in the channel, c, and at the resonance energy, ϵ_c; c) the reduced widths of the two wells, evaluated at the radius of the square-well, are equal in this channel and at this energy. One defines the "reflection factor", which accounts for the anomalous reflection of the square-well, as the ratio of the penetrability of the diffuse-edge well to that of the square-well at the square-well radius. If the many-body aspects of the nuclear problem have been accounted

for by choosing the diffuse-edge well to be an optical model potential, the imaginary term in the square-well potential is chosen to have the radius of the square-well and the depth of the diffuse-edge well. The electrostatic potential is chosen to be the same for both wells. The square-well defined in this manner is called the "equivalent square-well" (ESW).

In general, the parameters of the ESW are rather insensitive to the channel and the energy. Since the ESW and the corresponding one-body diffuse-edge well have the same penetrabilities and reduced widths, they are interchangeable in the one-body problem. It is seen from Eq. (3.5) that the spectroscopic factors should be rather insensitive to the nuclear size and surface since the nuclear reduced width and the one-body reduced width depend upon these aspects of the nucleus in a similar manner; in fact, we have checked this assertion in Table 6. Thus the spectroscopic factors, which account for the many-body aspects of the nuclear problem, should be about the same whether the nucleus is chosen to have the size and surface of the diffuse-edge well or of the corresponding ESW. Thus we can in a meaningful manner replace the conventional diffuse-edge nucleus with the equivalent square-edge nucleus for the purposes of analyzing decay rate, scattering, and absorption data.

5 - 2: APPLICATIONS TO HEAVY NUCLEI

In the present section, we will examine the validity of the equivalent square-edge nucleus model in heavy nuclei by considering the absorption of alpha-particles. The technique

employed is to evaluate the ESW for a fashionable optical model potential and then to study the dependence of the reflection factor upon the parameters of the problem by considering the transmission functions of the two one-body potential.

The one-body radial Schroedinger Equation, with an optical model potential, is of the form,

$$(5.1)\quad -\frac{\hbar^2}{2\nu}\frac{d^2u_c}{dR^2} + \left(V_C(R) + V_N(R) + iW_N(R) + \frac{\hbar^2}{2\nu}\frac{L(L+1)}{R^2}\right) = \epsilon_c u_c.$$

Defining the incoming wave in the channel, c, by,

$$(5.2)\quad I_c(R) = e^{-i\omega_c}\,(\bar{G}_c + i\bar{F}_c),$$

one has, at sufficiently large radius, that

$$(5.3)\quad \frac{u_c'(r)}{u_c(R)} \equiv C_c(R) + iD_c(R) = \frac{I_c'(R) - e^{2i(\alpha_c + i\beta_c)}\, I_c'(R)}{I_c(R) - e^{2i(\alpha_c + i\beta_c)}\, I_c(R)},$$

where C_c and D_c are the real and imaginary parts of the logarithmic derivative of u_c and where $\alpha_c + i\beta_c$ is the phase shift. In general, β_c is very small whence it is easily shown from Eq. (5.3) that,

$$(5.4)\quad T_c \doteq 4\beta_c \doteq \left.\frac{-4D_c}{(C_c\bar{G}_c - \bar{G}_c' - D_c\bar{F}_c)^2 + (\bar{F}_c' - C_c\bar{F}_c - D_c\bar{G}_c)}\right|_{R=R_m},$$

where T_c is the optical model transmission function and where R_m is sufficiently large that there is no further absorption due to the optical model potential.

If there is no absorption due to the optical model potential beyond the ESW radius, one can define,

(5.5) a) $P_{i_c} = -kR_{ESW}D_c$, $\quad \left(k = \frac{\sqrt{2\mu\epsilon_c}}{\hbar} \right)$

b) $S_{i_c} = -kR_{ESW}C_c$,

and write the optical model transmission function in the form (Preston (1962)),

$$(5.6) \qquad T_c = \frac{4P_c}{(S_c - S_{i_c})^2 + (P_c + iP_{i_c})^2} \frac{MR_o}{\hbar^2} \int_0^{R_o} W_N(R) \left| \frac{u_c(R)}{u_c(R_o)} \right|^2 dR.$$

Assuming u_c to be normalized in R_o, and noting that the surface thickness is small, one can write Eq. (5.6) in the form,

$$(5.7) \qquad T_c = \frac{4P_c}{(S_c - S_{i_c})^2 + (P_c + iP_{i_c})^2} \frac{W_o}{f_c(R_o)} ,$$

where,

$$(5.8) \qquad f_c(R_o) = \frac{\hbar^2}{mR_o} \left| u_c(R_o) \right|^2 .$$

Choosing the nuclear radius, R_o to be the ESW radius, and noting that, at resonance, $f(R_{ESW})$ is the one-body reduced width, one might expect in general that,

$$(5.9) \qquad \frac{f_{ESW}(R_{ESW})}{f_{diff}(R_{ESW})} \sim 1.$$

Numerical calculations show that the denominator, $(S_c - S_{i_c})^2 + (P_c + P_{i_c})^2$, is independent of the internal features of the well to within a few percent. Thus,

$$(5.10) \qquad \frac{T_{cdiff}}{T_{cESW}} \doteq \frac{P_{cdiff}}{P_{cESW}} .$$

It will be convenient to regard the transmission coefficient, T_c, of Eq. (5.4), as a function of the radius of evaluation, R_m. To study the effects of the imaginary potential within the barrier, one need then only consider the ratio of the transmission function of the diffuse-edge well to that

of the ESW. Within the barrier,

$$G_o >> F_o \quad ,$$

$$D << 1 \quad ,$$

so that,

$$(5.11) \quad g(R) \equiv \frac{T_{diff}(R)}{T_{ESW}(R)} = \frac{D_{diff}(R)}{D_{ESW}(R)} \quad .$$

One may then consider that the absorption due to the diffuse imaginary potential ceases where g(R) becomes asymptotic to the reflection factor, f.

From Eq. (5.1),

$$(5.12)\ a) \quad \frac{dC(R)}{dR} = k^2 \left(\frac{V_c}{\epsilon} + \frac{V_N}{\epsilon} - 1 \right) - C^2(R) - D^2(R),$$

$$b) \quad \frac{dD(R)}{dR} = \frac{k^2 W_N}{\epsilon} - 2C(R)\cdot D(R) \quad . \qquad (L = 0)$$

The solution of Eq. (5.12) b) in the barrier is of the form,

$$(5.13) \quad D(R) \propto \frac{KW_N}{\sqrt{\frac{V_c}{\epsilon} - 1}} + \text{constant} \cdot e^{-2k\sqrt{\frac{V_c}{\epsilon} - 1}\cdot R} \quad ,$$

since, in the barrier, D is very small and

$$C(R) \sim k\sqrt{\frac{V_C}{\epsilon} - 1} \quad .$$

If V_c/ϵ is sufficiently large, the first term dominates the second so that the absorption from the optical model potential exceeds that from the barrier.

The numerical example considered was that of s-wave scattering of an alpha-particle from a Pb^{208} target. The potential of the Pb^{208} target was taken to be of the form,

$$(5.14) \quad V_N(R) + iW_N(R) = (V_o + iW_o)\cdot\left(1 + \text{EXP}\left(\frac{R - r_o}{a}\right)\right)^{-1},$$

where the parameters where selected to be,

$$V_o = -99.58 \text{ MEV}; \quad r_o = 8.556 \text{ f.}; \quad a = 0.5 \text{ f.};$$

W_o = -10 MEV.

The corresponding ESW was found to have the parameters,

V_{ESW} = -99.99 MEV; R_{ESW} = 9.39 f.; W_{ESW} = -10 MEV;

f = 1.9;

at an incident relative energy of 8.9795 MEV (Po^{212} decay energy). The technique employed was to solve the coupled differential equations, Eqs. (5.12) a) and b), for C and D.

The effects of the height of the Coulomb barrier are illustrated in Figure 8. It is seen that, for heavy nuclei, the transmission of the barrier is very sensitive to the tail of the imaginary potential within the barrier. This long-range absorption is an intrinsic property of all optical model calculations, even though it may not have a good physical basis. Where it becomes dominant, a modification of the absorptive potential (to remove its tail) shall be considered.

In Figure 9, the imaginary part of the diffuse-edge potential has been chosen to be the same as that of the ESW. A reflection factor of 1.9 is obtained at the alpha-decay energy of 8.9795 MEV, comparing with a value of 2.0 obtained by analytic calculation of the penetrabilities as discussed in Chapter 3. The value of the reflection factor was found to be rather insensitive to the height of the Coulomb barrier; from this, and noting that it does not depend sensitively upon the energy, it is seen that the ESW parameters should be rather insensitive to the decay channel and energy. It was also found to be insensitive to the strength of the imaginary part of the optical model potential.

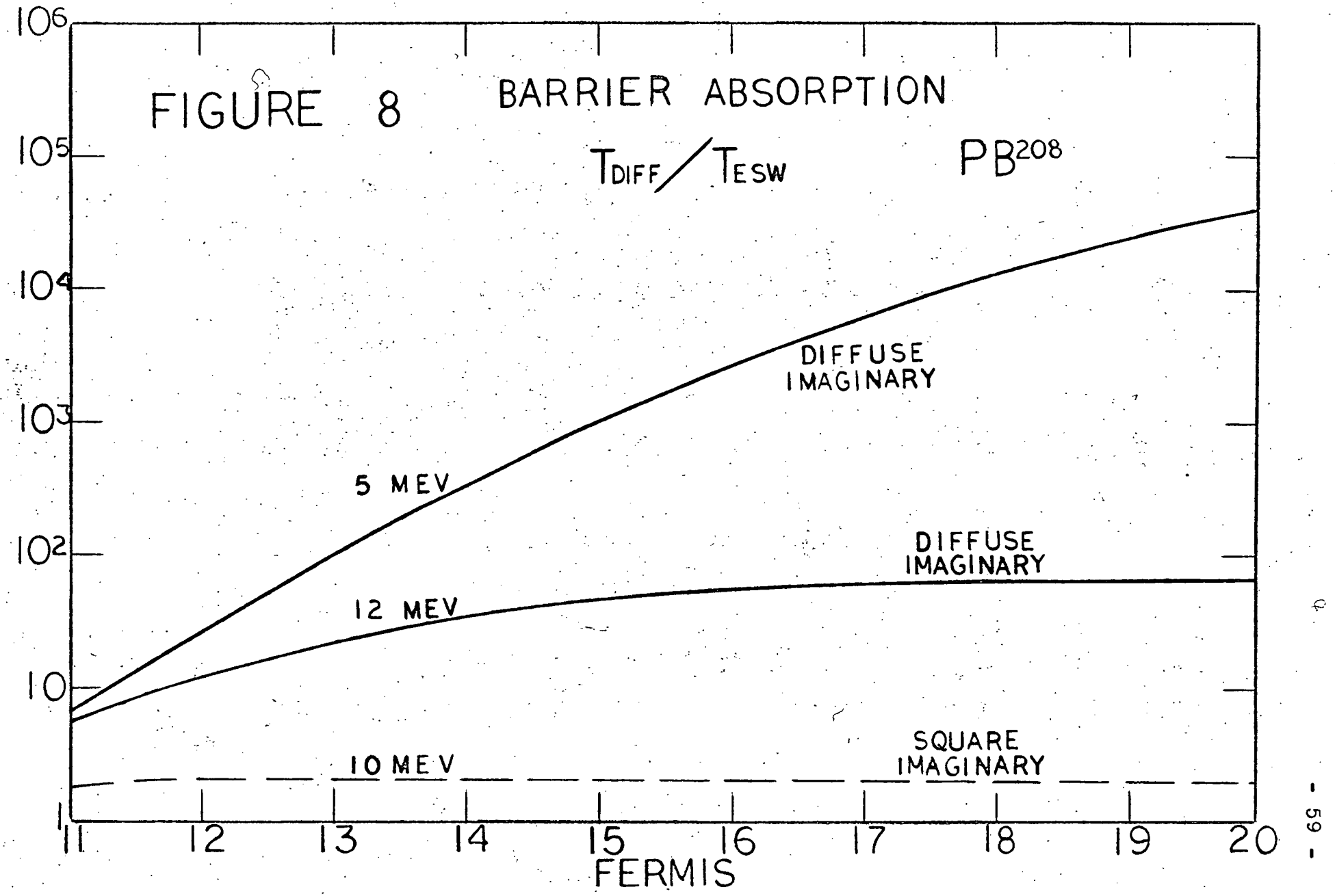
FIGURE 8
BARRIER ABSORPTION
T_{DIFF}/T_{ESW}
PB^{208}
10^6
10^5
10^4
10^3
10^2
10
1
DIFFUSE IMAGINARY
5 MEV
DIFFUSE IMAGINARY
12 MEV
10 MEV
SQUARE IMAGINARY
11
12
13
14
15
16
17
18
19
20
FERMIS

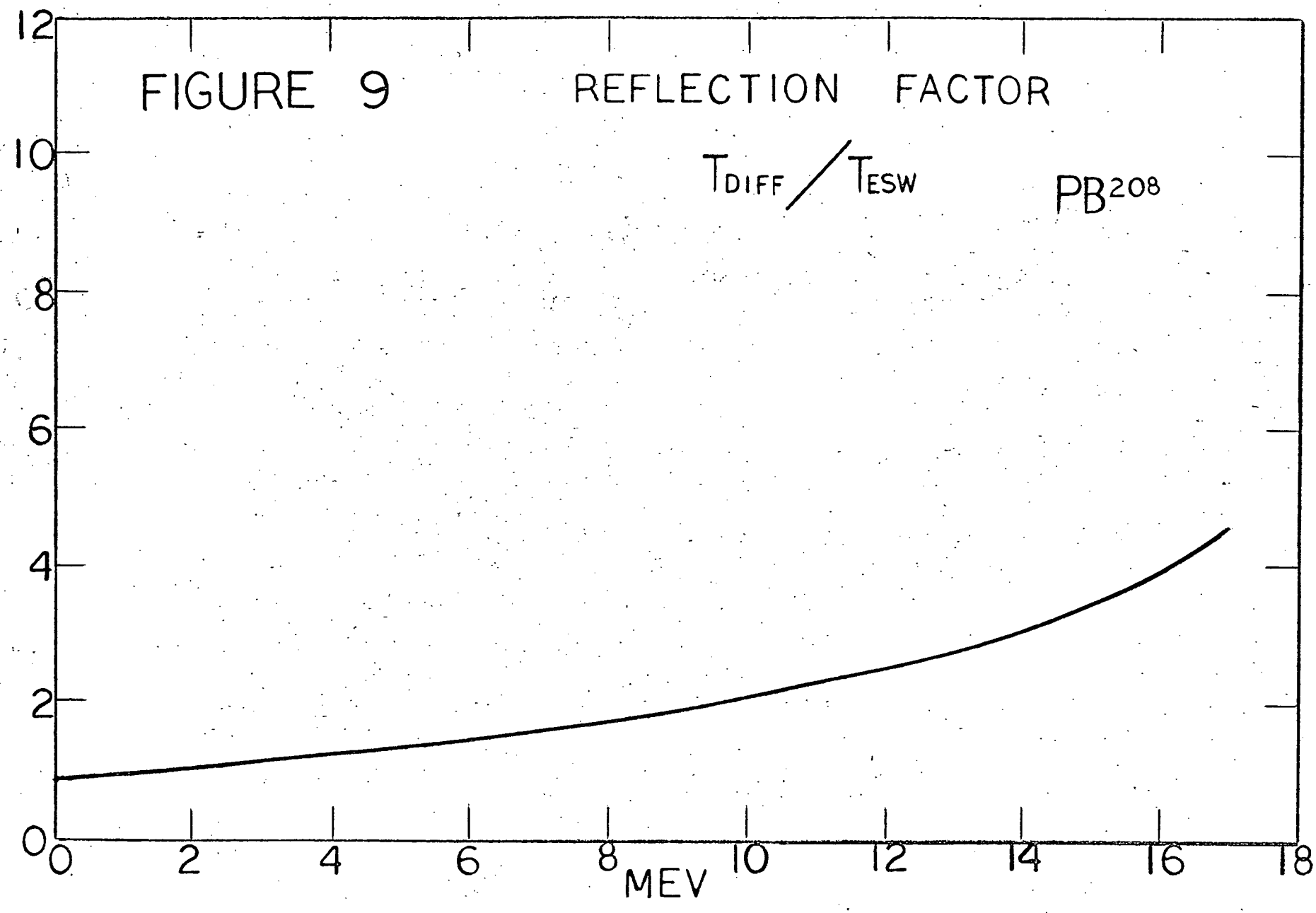
FIGURE 9
REFLECTION FACTOR
T_{DIFF} / T_{ESW}
PB^{208}
12
10
8
6
4
2
0
0
2
4
6
8
10
12
14
16
18
MEV

In the calculation of Vogt, Michaud, and Reeves (1965), the diffuse-edge optical model potential was chosen to have a diffuse complex part. They obtain a value of 4.62 for the reflection factor; replacing the diffuse-edge complex part by the complex part of the appropriate ESW yields a value of 2.8. It might, therefore, seem that the reflection factor has been overestimated by a factor of two. They also state a reflection factor of 100 when the ESW is replace with a square-well having the same radius as the diffuse-edge well. In the present calculation, the ratio of the penetrability of the diffuse-edge well to a square-well was found to vary rather slowly with the radius selected.

It is seen from the example studied in this Chapter that the radius of the ESW is about a fermi larger than that of the corresponding diffuse-edge well. It is apparent from Harada's calculation that he has, essentially, used such an ESW for calculating the independent-particle model reduced widths. Thus the large radius in his calculation is consistent with conventional nuclear sizes, provided that it is interpreted as the radius of an equivalent square-edge nucleus.

CHAPTER 6 CONCLUSIONS

In this thesis we have shown that much of the discrepancy between the empirical alpha-particle decay rates of heavy nuclei and those estimated from nuclear shell-model calculations can be removed by a more direct treatment of the nuclear surface. We have contended that previous calculations on alpha-particle decay rates have essentially used the equivalent square-edge nucleus model of Vogt; we have shown by considering the one-body problem that the equivalent square-edge nucleus has a considerably larger radius than the diffuse-edge nucleus to which it corresponds. We have concluded that the large radii which were found necessary in previous calculations on alpha-particle decay rates to obtain agreement with the empirical values were the radii of the equivalent square-edge nucleus model rather than the actual radii of the decaying systems being considered. In fact, we have shown that the radii of the corresponding diffuse-edge nuclei agree with the conventional radii believed to be typical of a heavy nucleus.

In our calculations, we have checked that the J.W.K.B. and the square-well estimates of the nuclear penetrability used by previous authors are in reasonable agreement with the analytic values. In fact, we have found in Chapter 3 that the J.W.K.B. estimate is quite good to within about one-tenth of a fermi of the classical inner turning point and that the square-well estimate differs by less than an order of magnitude at the classical inner turning point.

We have demonstrated in Chapter 4 that the one-body reduced widths appropriate to the decay of Po^{212} are enhanced considerably by a diffuse nuclear edge. In fact, we have checked the effect on the one-body decay constant directly by calculating the differential elastic scattering cross-section for the one-body scattering of an alpha-particle from Pb^{208} at 90^{o}_{CM}. We have included the many-body aspects of the problem by repeating the calculation of Harada with the square-well one-body wave functions of his calculation being replaced with the resonant wave functions of a diffuse-edge well. We have found that his square-well calculation corresponds to a diffuse-edge well calculation of a smaller and more conventional nuclear radius. In fact, we have contended that his calculation corresponds to the equivalent square-edge nucleus calculation for such a diffuse-edge well.

We have examined the dependence of the equivalent square-edge nucleus model parameters in Chapter 5 by calculating the one-body transmission functions for the absorption of an alpha-particle by a Pb^{208} nucleus. We have found that, provided the tail of the imaginary part of the optical model potential is truncated at the nuclear radius, the equivalent square-edge nucleus model parameters are rather insensitive to the nature of the reaction and to the many-body aspects of the problem. We have from this concluded that the equivalent square-edge nucleus model should have some validity in heavy nuclei.

We have interpreted the results of our calculations as suggesting that the independent-particle model, with only

those correlations introduced by configuration mixing, can satisfactorily account for the clustering into complex particles in the nuclear surface; in particular, we believe that such a model can predict reasonable values for the alpha-particle decay rates of heavy nuclei.

BIBLIOGRAPHY

Arima, A., and Terasawa, T., "Progress of Theoretical Physics 23, 115" (1960).

Bencze, Gy., and Sandelescu, A., "Physics Letters 22, 473" (1966).

Ford, K.W., and Hill, D.L., "Annual Review of Nuclear Science 5, 25" (1955).

Harada, K., "Progress of Theoretical Physics 26, 667" (1961).

Igo, G., "Physical Review 115, 1665" (1959).

Mang, H.J., "Physical Review 119, 1069" (1960).

Mang, H.J., "Annual Review of Nuclear Science 14, 1" (1964)

Messiah, A., "Quantum Mechanics, Volume I" (1962). (John Wiley & Sons, Inc., New York)

Noya, H., Arima, A., and Horie, H., "Progress of Theoretical Physics, Supplement No. 8, 33" (1959).

Preston, M.A., "Physics of the Nucleus" (1962). (Addison-Wesley, Reading, Mass.)

Rasmussen, J.O., "Physical Review 113, 1593" (1959).

Rose, M.E., "Elementary Theory of Angular Momentum" (1957). (John Wiley & Sons, Inc., New York)

Talmi, I., "Helvetica Physica Acta 25, 185" (1952).

Thomas, R.G., "Progress of Theoretical Physics 12, 253" (1954).

Vogt, E.W., "Reviews of Modern Physics 34, 723" (1962).

Vogt, E.W., Michaud, G., and Reeves, H., "Physics Letters 19, 570" (1965).

Wilkinson, D.H., "Proceedings of the Rutherford Conference on Nuclear Structure, 339" (1961).

Zeh, H.-D., and Mang, H.J., "Nuclear Physics 29, 529" (1962).

Zeh, H.-D., "Zeitschrift fur Physik 175, 490" (1963).

APPENDIX A HARADA'S FORMULA FOR THE REDUCED WIDTHS FOR ALPHA-PARTICLE DECAY IN EVEN-EVEN NUCLEI

Harada (1961) has derived a convenient formula for evaluating the independent-particle model reduced widths for the ground state alpha-particle decay transition in even-even nuclei with the use of harmonic oscillator one-nucleon wave functions. In this appendix, we present an outline of the derivation of his result.

The reduced width amplitude for alpha-particle decay has been defined in Eq. (3.3),

$$(3.3)\quad \gamma_c = \sqrt{\frac{h^2 R_o}{2}} \int_{\Omega, \underline{\xi}, \underline{x}_\sigma, \underline{s}} \Psi_o^* \mathcal{X} \sum_{m_j M_L} \langle jL m_j M_L | JM \rangle \Psi^\tau_{jm_j} \cdots$$
$$\cdots Y_L^{M_L} \, d\Omega d\underline{\xi} d\underline{x}_\sigma d\underline{s} \quad , \#$$

where: Ψ_o is the parent nucleus wave function; $\mathcal{X}$ is the alpha-particle wave function;, $\Psi^\tau_{jm_j}$ is the daughter nucleus wave function; $Y_L^{M_L}$ is the spherical harmonic describing the relative motion of the decay fragments. Here, $\mathcal{X}$ and $\Psi^\tau_{jm_j}$ are assumed to be properly antisymmetrized and Ψ_o is assumed to be partially antisymmetrized in the sense defined in Chapter 2.

We assume the parent nucleus and daughter nucleus to be even-even nuclei and to be represented by independent-particle model wave functions of seniority zero. We consider only the ground state transitions, so that the parent nucleus, daughter nucleus, and the alpha-particle have zero angular momentum; the relative orbital angular momentum of the decay fragments is then also zero.

The notation is that of Chapter 2 and Chapter 3.

It is convenient to expand the parent nucleus wave function in the two-proton and the two-neutron wave functions which can be formed from the unfilled subshell of the parent nucleus configuration; it is these nucleons which we expect to contribute to alpha-decay.

In order to make the above expansion, we require the double parentage coefficients, $(j^{m-2}(sj)j^2(J')J\{\} j^mSJ)$. Here, j^m denotes the angular momenta of the m one-nucleon wave functions of the unfilled subshell of the parent configuration; j^2 denotes the angular momenta of the two one-nucleon wave functions of the unfilled subshell which are taken to constitute the two-nucleon wave function; j^{m-2} denotes the angular momenta of the remaining m-2 one-nucleon wave functions of the daughter configuration. S and J are the seniority and the total angular momentum of the parent nucleus, respectively; s and j are the seniority and the total angular momentum of the daughter nucleus, respectively; J' is the total angular momentum of the two-nucleon system formed from the unfilled subshell.

Noting the partial antisymmetrization of Ψ_o, using the subscripts 1 and 3 to denote proton and neutron quantum numbers, respectively, and invoking our previous assumptions,

$$(A.1)\quad \int_{\underline{x}_6,\underline{s}_6} \Psi_o \, \psi_{oo}^{j_p^{A_1-2} \, o \, j_n^{A_3-2} \, o} \, d\underline{x}_6 d\underline{s}_6 = \cdots$$

$$\cdots = \int_{\underline{x}_6,\underline{s}_6} \Big[\sum (j_p^{A_1-2}(s_1 j_1) j_p^2(J_1')0\{\} j_p^{A_1} 00)$$

$$\cdots (j_n^{A_3-2}(s_3 j_3) j_n^2(J_3')0\{\} j_n^{A_3} 00) \left[\binom{A_1}{2} \binom{A_3}{2} \right]^{-\frac{1}{2}}$$

$$\cdots \phi_p(j_p^2, J_1')\,\phi_n(j_n^2, J_3')\,\Big\}^{j_p^{A_1-2}\ s_1\ j_n^{A_3-2}\ s_3}_{jm_j}$$

$$\cdots \Big\}^{j_p^{A_1-2}\ o\ j_n^{A_3-2}\ o}_{oo} \Big] d\underline{x}_\sigma d\underline{s}_\sigma$$

$$= \sum (j_p^{A_1-2}(00) j_p^2(0)0 \,|\, j_p^{A_1} 00)\,(j_n^{A_3-2}(00) j_n^2(0)0 \,|\, j_n^{A_3} 00)$$

$$\cdots \left[\binom{A_1}{2}\binom{A_3}{2}\right]^{-\frac{1}{2}} \phi_p(j_p^2, 0)\,\phi_n(j_n^2, 0)$$

$$= \left[\binom{A_1}{2}\binom{A_3}{2}\right]^{\frac{1}{2}} (j_p^{A_1-2}(00) j_p^2(0)0 \,|\, j_p^{A_1} 00)\,(j_n^{A_3-2}(00) j_n^2(0)0 \,|\, j_n^{A_3} 00)$$

$$\cdots \phi_p(j_p^2, 0)\,\phi_n(j_n^2, 0)$$

$$= \left[\binom{A_1}{2}\binom{A_3}{2}\right]^{\frac{1}{2}} \left[\frac{(2j_1 + 3 - A_1)}{(A_1 - 1)(2j_1 + 1)}\right]^{\frac{1}{2}} \left[\frac{(2j_3 + 3 - A_3)}{(A_3 - 1)(2j_3 + 1)}\right]^{\frac{1}{2}} \phi_p(j_p^2, 0)\,\phi_n(j_n^2, 0).$$

Here, ϕ_p (ϕ_n) depends only upon the proton (neutron) co-ordinates, ($\underline{x}_1$, $\underline{x}_2$) (($\underline{x}_3$, $\underline{x}_4$)); A_1 (A_3) denotes the number of protons (neutrons) in the unfilled proton (neutron) subshell, j_p (j_n), of the parent configuration, the angular momenta of the protons (neutrons) in this subshell being denoted by j_1 (j_3). In the first step of Eq. (A.1), we have expanded the parent nucleus wave function in the two-proton (two-neutron) wave functions of the unfilled subshell; $\left[\binom{A_1}{2}\binom{A_3}{2}\right]^{-\frac{1}{2}}$ is a normalization factor accounting for the fact that the two protons (neutrons) may be selected from the unfilled proton (neutron) subshell in $\binom{A_1}{2}$ ($\binom{A_3}{2}$) ways. In the second step, the integration has been performed; in the third step, we have summed over the ways of selecting two protons (neutrons) from the unfilled proton (neutron) subshell. In the final step, we have noted the result of Noya, Arima, and Horie (1959),

$$(A.2) \quad (j^{m-2}(00) j^2(0)0 \,|\, j^m 00) = \left[\frac{(2j + 3 - m)}{(m-1)(2j\ 1)}\right]^{\frac{1}{2}} .$$

Noting,

$$Y_0^0 = (4\pi)^{-\frac{1}{2}} ,$$

and Eq. (A.1), and writing,

$$(A.3)\quad S_{j_1 j_3}^{A_1 A_3} = \left[\binom{A_1}{2}\binom{A_3}{2}\right]^{\frac{1}{2}} \left[\frac{(2j_1+3-A_1)}{(A_1-1)(2j_1+1)}\right]^{\frac{1}{2}} \left[\frac{(2j_3+3-A_3)}{(A_3-1)(2j_3+1)}\right]^{\frac{1}{2}},$$

Eq. (3.3) becomes,

$$(A.4)\quad \gamma_\alpha = \frac{1}{\sqrt{4\pi}} \sqrt{\frac{h^2 R_0}{2\mu}}\, S_{j_1 j_3}^{A_1 A_3} \int_{\Omega,\underline{\xi},\underline{s}_\alpha} \phi_p(j_p^2,0)\, \phi_n(j_n^2,0)\, \chi\, d\Omega\, d\underline{\xi}\, d\underline{s}_\alpha .$$

We have defined the alpha-particle wave function, , in Chapter 4:

$$(4.8)\quad \chi(1234) = \left(\frac{\beta^{3/2}}{(\frac{1}{2}!)}\right)^{3/2} \mathrm{EXP}\left(-\frac{\beta}{2}\left(\frac{\xi_1^2}{2} + \frac{\xi_2^2}{2} + \xi_3^2\right)\right)$$

$$\cdots (4\pi)^{-3/2} \chi_o^o(12)\, \chi_o^o(34).$$

To perform the integration in Eq. (A.4) it is, therefore, convenient to transform the proton and the neutron wave functions to the L - S representation and to then transform the proton and neutron co-ordinates to the internal and relative co-ordinates of the alpha-particle.

To see the manner in which to transform the two-nucleon wave functions to the L - S representation, we consider only the j - j coupled two-proton wave function, $\phi_p(j_p^2,0)$. (The neutron case is analogous.)

j - j representation:	L - S representation:
$\underline{j}_1^{(1)} = \underline{l}_1^{(1)} + \underline{s}_1^{(1)}$;	$\underline{L} = \underline{l}_1^{(1)} + \underline{l}_1^{(2)}$;
$\underline{j}_1^{(2)} = \underline{l}_1^{(2)} + \underline{s}_1^{(2)}$;	$\underline{S} = \underline{s}_1^{(1)} + \underline{s}_1^{(2)}$;
$\underline{J} = \underline{j}_1^{(1)} + \underline{j}_1^{(2)} = 0$;	$\underline{J} = \underline{L} + \underline{S} = 0$;

the superscript (1) or (2) denotes the first or second proton, respectively. Both the j - j coupled wave functions and the

#Harada employs the co-ordinates $\underline{\xi}_{1H} = \frac{1}{2}\underline{\xi}_1$; $\underline{\xi}_{2H} = \frac{1}{2}\underline{\xi}_2$; $\underline{\xi}_{3H} = \underline{\xi}_3$.

L - S coupled wave functions form complete sets so that we may make the expansion,

$$\left|(l_1^{(1)}s_1^{(1)})j_1^{(1)},(l_1^{(2)}s_1^{(2)})j_1^{(2)};\ JM\right\rangle =$$

$$\sum_{L,S}\left\langle(l_1^{(1)}l_1^{(2)})L,(s_1^{(1)}s_1^{(2)})S;JM\middle|(l_1^{(1)}s_1^{(1)})j_1^{(1)},(l_1^{(2)}s_1^{(2)})j_1^{(2)};JM\right\rangle$$

$$\cdots\left|(l_1^{(1)}l_1^{(2)})L,(s_1^{(1)}s_1^{(2)}S;\ JM\right\rangle\ .$$

We adopt the notation of Rose (1957):

$$T(LS;j_1^{(1)}j_1^{(2)}) \equiv$$

$$\left\langle(l_1^{(1)}l_1^{(2)})L,(s_1^{(1)}s_1^{(2)})S;JM\middle|(l_1^{(1)}s_1^{(1)})j_1^{(1)},(l_1^{(2)}s_1^{(2)})j_1^{(2)};JM\right\rangle.$$

From Eq. (4.8), only that matrix element for which $\underline{S} = 0$ (and, hence, $\underline{L} = 0$) can contribute to the integral in Eq. (A.4). We need, therefore, only consider coefficients of the form, $T(00;jj)$. We evaluate this coefficient by first expressing it in terms of a 9-j symbol:

$$T(00;jj) = (2j+1)\begin{Bmatrix} 1 & 1 & 0 \\ \frac{1}{2} & \frac{1}{2} & 0 \\ j & j & 0 \end{Bmatrix} ;$$

the 9-j symbol can be reduced to a W coefficient (or a 6-j symbol) which is readily evaluated. Conforming with Harada, we write the solution in the form,

$$(A.5)\quad T(00;jj) = \frac{(-1)^{1+\frac{1}{2}-j}}{\sqrt{2}}(2j+1)W(jljl;\tfrac{1}{2}0)\ ^{\#}$$

$$= \frac{1}{\sqrt{2}}\sqrt{\frac{2j+1}{2l+1}}\ .$$

We write Eq. (A.4) in the L - S coupled scheme as,

#The value of the matrix elements, $T(00;jj)$, stated by Harada contains a misprint (being in error by a factor of $1/\sqrt{2}$). This error does not appear to have been carried through in his subsequent calculations.

$$(A.6) \qquad = \frac{1}{\sqrt{4\pi}} \sqrt{\frac{h^2 R_0}{2\mu}} \, S^{A_1 A_3}_{j_1 j_3} \, T(00;j_1 j_1) T(00;j_3 j_3) \int_{\Omega, \underline{\xi}, \underline{s}_\alpha} \phi_p(\underline{L}=0, \underline{S}=0)$$

$$\cdots \phi_n(\underline{L}=0, \underline{S}=0) \chi \, d\Omega d\underline{\xi} d\underline{s}_\alpha \, .$$

The one-nucleon wave functions are taken to be harmonic oscillator wave functions:

$$(A.7) \quad \phi^m_{nlj}(\underline{r}, \underline{s}) = \psi_{nl}(r) \sum_\mu \langle l \tfrac{1}{2} \mu m-\mu \,|\, jm \rangle Y^{m-\mu}_l\left(\frac{\underline{r}}{r}\right) \chi^{m-\mu}_{\frac{1}{2}} \, ,$$

where,

$$(A.8) \quad \psi_{nl}(r) = \sqrt{\frac{2n! b^{3/2}}{(n+l+\frac{1}{2})!}} \, L_n^{l+\frac{1}{2}}(br^2) (\sqrt{b} r)^l e^{-\frac{1}{2} b r^2} \, ;$$

$$L_n^{l+\frac{1}{2}}(br^2) = \sum_{h=0}^{n} \binom{n+l+\frac{1}{2}}{n-h} \frac{(-1)^h}{h!} (br^2)^h \, .$$

(b is the harmonic oscillator size parameter.) Then,

$$(A.9) \quad \text{i)} \quad \phi_p(\underline{L}=0, \underline{S}=0) = \psi_{\nu_1 l_1}(x_1) \psi_{\nu_1 l_1}(x_2) \sum_{\mu_1} \langle l_1 l_1 \mu_1 - \mu_1 \,|\, 00 \rangle$$

$$\cdots Y_{l_1}\left(\frac{\underline{x}_1}{x_1}\right) Y_{l_1}\left(\frac{\underline{x}_2}{x_2}\right) \chi^0_0(12) \, ;$$

$$\text{ii)} \quad \phi_n(\underline{L}=0, \underline{S}=0) = \psi_{\nu_3 l_3}(x_3) \psi_{\nu_3 l_3}(x_4) \sum_{\mu_3} \langle l_3 l_3 \mu_3 - \mu_3 \,|\, 00 \rangle$$

$$\cdots Y_{l_3}\left(\frac{\underline{x}_3}{x_3}\right) Y_{l_3}\left(\frac{\underline{x}_4}{x_4}\right) \chi 8(34) \, ;$$

ν_1 and l_1 (ν_3 and l_3) are the principal and orbital quantum numbers, respectively, of the unfilled proton (neutron) subshell.

To evaluate the integrals in Eq. (A.6), it is convenient to write the co-ordinates, $\underline{\xi}_i$, in terms of their radial and angular components, ξ_i and Ω_i, respectively. It is also convenient to define the co-ordinates,

$$\underline{r}_{12} = \tfrac{1}{2}(\underline{x}_1 + \underline{x}_2); \qquad \underline{r}_{34} = \tfrac{1}{2}(\underline{x}_3 + \underline{x}_4).$$

Expressing the two-proton and the two-neutron wave functions in terms of these co-ordinates,

(A.10) i) $$\psi_{\nu_1 l_1}(x_1)\psi_{\nu_1 l_1}(x_2)\sum_{\mu_1}\langle l_1 l_1 \mu_1 -\mu_1 | 00\rangle Y_{l_1}^{\mu_1}\left(\frac{x_1}{x_1}\right)Y_{l_1}^{-\mu_1}\left(\frac{x_2}{x_2}\right)$$

$$= \sum_{\substack{N_1,\bar{L}_1,\\ n_1,\bar{l}_1,}} \langle N_1 \bar{L}_1 n_1 \bar{l}_1; 0 | \nu_1 l_1 \nu_1 l_1; 0\rangle \psi_{N_1\bar{L}_1}(r_{12})$$

$$\cdots \psi_{n_1\bar{l}_1}(\xi_1)\sum_{\bar{\mu}_1}\langle \bar{L}_1 \bar{l}_1 -\bar{\mu}_1 \bar{\mu}_1 | 00\rangle Y_{\bar{L}_1}^{-\bar{\mu}_1}\left(\frac{r_{12}}{r_{12}}\right)Y_{\bar{l}_1}^{\bar{\mu}_1}(\Omega_1) \quad ;^{\#}$$

ii) $$\psi_{\nu_3 l_3}(x_3)\psi_{\nu_3 l_3}(x_4)\sum_{\mu_3}\langle l_3 l_3 \mu_3 -\mu_3 | 00\rangle Y_{l_3}^{\mu_3}\left(\frac{x_3}{x_3}\right)Y_{l_3}^{-\mu_3}\left(\frac{x_4}{x_4}\right)$$

$$= \sum_{\substack{N_2,\bar{L}_2,\\ n_2,\bar{l}_2}} \langle N_2 \bar{L}_2 n_2 \bar{l}_2; 0 | \nu_3 l_3 \nu_3 l_3; 0\rangle \psi_{N_2\bar{L}_2}(r_{34})\psi_{n_2\bar{l}_2}(\xi_2)$$

$$\cdots \sum_{\bar{\mu}_2}\langle \bar{L}_2 \bar{l}_2 -\bar{\mu}_2 \bar{\mu}_2 | 00\rangle Y_{\bar{L}_2}^{-\bar{\mu}_2}\left(\frac{r_{34}}{r_{34}}\right)Y_{\bar{l}_2}^{\bar{\mu}_2}(\Omega_2) \quad .$$

Substituting Eqs. (A.9) and (A.10) into Eq. (A.6), and integrating over Ω_1 and Ω_2,

(A.11) $$\gamma_\alpha = \sqrt{4\pi}\sqrt{\frac{h^2 R_o}{2}}\; S_{j_1 j_3}^{A_1 A_3}\, T(00; j_1 j_1) T(00; j_3 j_3)$$

$$\cdots \int_{\Omega, \xi_1, \xi_2, \underline{\xi}_3, \underline{s}_\alpha} \sum_{n_1, n_2} \langle N_1 0 n_1 0; 0 | \nu_1 l_1 \nu_1 l_1; 0\rangle$$

$$\cdots \langle N_2 0 n_2 0; 0 | \nu_3 l_3 \nu_3 l_3; 0\rangle \psi_{N_1 0}(r_{12})\; Y_0^0\left(\frac{r_{12}}{r_{12}}\right)$$

$$\cdots \psi_{N_2 0}(r_{34})\; Y_0^0\left(\frac{r_{34}}{r_{34}}\right)\chi_o^o(12)\chi_o^o(34)\psi_{n_1 0}(\xi_1)$$

$$\cdots \psi_{n_2 0}(\xi_2)\chi\, d\omega\, \xi_1^2 d\xi_1 \xi_2^2 d\xi_2 d\underline{\xi}_3 d\underline{s}_\alpha \quad .$$

Noting,

(A.12) $$\psi_{N_1 0}(r_{12})Y_0^0\left(\frac{r_{12}}{r_{12}}\right)\psi_{N_2 0}(r_{34})Y_0^0\left(\frac{r_{34}}{r_{34}}\right) = \cdots$$

$$\cdots = \sum_{n_3}\langle N 0 n_3 0; 0 | N_1 0 N_2 0; 0\rangle \psi_{N0}(R_o)Y_0^0(\Omega)\,\psi_{n_3 0}(\xi_3)$$

$$\cdots Y_0^0(\Omega_3) \quad ,$$

#The Talmi transformation coefficients, $N_1 L_1 N_2 L_2; L\; n_1 l_1 n_2 l_2; L$, are defined and evaluated in Appendix B.

substituting Eq. (4.8) and Eq. (A.12) into Eq. (A.11), and integrating over $_3$ and ,

$$(A.13)\quad \gamma_\alpha = \sqrt{\frac{h^2 R_o}{2}}\, S^{A_1 A_3}_{j_1 j_3}\, \mathcal{O}(R_o) \ ,$$

where,

$$(A.14)\quad \mathcal{O}(R_o) = T(00;j_1 j_1)T(00;j_3 j_3)\left(\frac{\beta^{3/2}}{(\frac{1}{2}!)}\right)^{3/2}$$

$$\cdots \sum_{n_1,n_2,n_3} \langle N0n_3 0;0|N_1 0 N_2 0;0\rangle \langle N_1 0 n_1 0;0|\mathcal{V}_1 l_1 \mathcal{V}_1 l_1;0\rangle$$

$$\cdots \langle N_2 0 n_2 0;0|\mathcal{V}_3 l_3 \mathcal{V}_3 l_3;0\rangle \int_0^\infty \psi_{n_1 0}(\xi_1)\,\mathrm{EXP}(-\tfrac{\beta}{2}\tfrac{\xi_1^2}{2})\xi_1^2 d\xi_1$$

$$\cdots \int_0^\infty \psi_{n_2 0}(\xi_2)\,\mathrm{EXP}(-\tfrac{\beta}{2}\tfrac{\xi_2^2}{2})\xi_2^2 d\xi_2$$

$$\cdots \int_0^\infty \psi_{n_3}(\xi_3)\,\mathrm{EXP}(-\tfrac{\beta}{2}\xi_3^2)\xi_3^2 d\xi_3 \cdot \psi_{N0}(R_o) \ .$$

Performing the integrations in Eq. (A.14), we can write the overlap integral in the form,

$$(A.15)\quad \mathcal{O}(R_o) = \sum_N \mathcal{O}_N(R_o) \ ,$$

where,

$$(A.16)\quad \mathcal{O}_N(R_o) = T(00;j_1 j_1)T(00;j_3 j_3) \sum_{n_1,n_2} \langle N0n_3 0;0|N_1 0 N_2 0;0\rangle$$

$$\cdots \langle N_1 0 n_1 0;0|\mathcal{V}_1 l_1 \mathcal{V}_1 l_1;0\rangle \langle N_2 0 n_2 0;0|\mathcal{V}_3 l_3 \mathcal{V}_3 l_3;0\rangle$$

$$\cdots (\tfrac{1}{2}!)^{-\frac{3}{2}} \left[\frac{(n_1+\frac{1}{2})!(n_2+\frac{1}{2})!(n_3+\frac{1}{2})!}{n_1!n_2!n_3!}\right]^{\frac{1}{2}} \left(\frac{2\sqrt{\beta b}}{\beta+b}\right)^{9/2}$$

$$\cdots \left(\frac{\beta-b}{\beta+b}\right)^{n_1+n_2+n_3} \psi_{N0}(R_o) \ .$$

The reduced width can now be calculated from Eq. (A.13) and Eq. (A.16).

APPENDIX B TALMI TRANSFORMATION COEFFICIENTS

The Talmi transformation coefficients are the transformation coefficients for expanding the shell model wave function of a two-particle system in terms of the wave function of their relative and center-of-mass co-ordinates. If the average field is taken to be an harmonic oscillator well, these coefficients can be calculated in a simple manner. In this appendix, a recursive relation is derived which is convenient for the computer evaluation of those Talmi coefficients which have been used in Chapter 4 and Appendix A. A more general recursive relation for the Talmi coefficients appropriate to an harmonic oscillator well has been derived by Arima and Terasawa (1959), and the technique employed in the present discussion is based upon their calculation.

In the discussion to follow, the wave functions discussed will be assumed to be harmonic oscillator functions. The spatial harmonic oscillator functions are of the form,

$$(B.1)\quad \phi^{\nu}_{\nu_1}(\underline{r},b) = \psi_{\nu_1}(r,b)Y^{\nu}_{1}(\Omega),$$

where: r and Ω are the radial and angular components of $\underline{r}$, respectively; Y^{ν}_{1} is a spherical harmonic; b is the harmonic oscillator size parameter; $\psi_{\nu_1}(r,b)$ is the radial harmonic oscillator function defined in Eq. (A.8).

The spatial single-particle states will be taken to be $\phi^{\nu_1}_{1 l_1}(\underline{r}_1,b)$ and $\phi^{\nu_2}_{2 l_2}(\underline{r}_2,b)$. The spatial wave function of the two particles is then,

$$(B.2)\quad \phi^{\overline{LM}}_{\nu_1 l_1 \nu_2 l_2}(\underline{r}_1,\underline{r}_2,b) = \psi_{\nu_1 l_1}(r_1,b)\psi_{\nu_2 l_2}(r_2,b) \cdots \sum_{\nu_1,\nu_2} \langle l_1 l_2 \nu_1 \nu_2 | \overline{LM} \rangle \; Y^{\nu_1}_{l_1}(\Omega_1)\, Y^{\nu_2}_{l_2}(\Omega_2).$$

The relative co-ordinate and the center-of-mass co-ordinate will be denoted by,

$$\underline{r} = \underline{r}_1 - \underline{r}_2; \qquad \underline{R} = \tfrac{1}{2}(\underline{r}_1 + \underline{r}_2);$$

respectively. The one-particle wave function in the relative co-ordinate will be denoted by $\phi^m_{nl}(\underline{r},c)$, and the one-particle wave function in the center-of-mass by $\phi^M_{NL}(\underline{R},C)$. It is easily shown that,

$$c = \tfrac{1}{2}b; \qquad C = 2b.$$

One can construct the two-particle wave functions from the relative and center-of-mass wave functions:

$$(B.3) \quad \Phi^{\overline{LM}}_{NLnl} = \phi_{NL}\,\phi_{nl} \sum_{M,m} \langle Llm\,|\,\overline{LM}\rangle\, Y^M_L\, Y^m_l \ .$$

Since both the set of two-particle states defined by Eq. (B.2) and that defined by Eq. (B.3) are complete, we can make the expansion,

$$(B.4) \quad i) \ \Phi^{\overline{LM}}_{\nu_1 l_1 \nu_2 l_2} = \sum_{\substack{N,L,n,\\ l,\overline{L}',\overline{M}'}} \langle NLnl;\overline{L}'\overline{M}'\,|\,\nu_1 l_1 \nu_2 l_2;LM\rangle\, \Phi^{\overline{L}'\overline{M}'}_{NLnl} \ ;$$

$$ii) \ \Phi^{\overline{LM}}_{NLnl} = \sum_{\substack{\nu_1,l_1,\\ \nu_2,l_2,\\ \overline{L}',\overline{M}'}} \langle \nu_1 l_1 \nu_2 l_2;\overline{L}'\overline{M}'\,|\,NLnl;LM\rangle\, \Phi^{\overline{L}'\overline{M}'}_{\nu_1 l_1 \nu_2 l_2} \ ;$$

where $\langle NLnl;\overline{L}'\overline{M}'\,|\,\nu_1 l_1 \nu_2 l_2;\overline{LM}\rangle$ and $\langle \nu_1 l_1 \nu_2 l_2;\overline{L}'\overline{M}'\,|\,NLnl;\overline{LM}\rangle$ are expansion coefficients. The properties of these coefficients were first studied by Talmi, and the coefficients bear his name (Talmi (1952)).

To derive a formula for the Talmi coefficients, we follow the procedure of Arima and Terasawa (1959). We first note that, from conservation of energy,

(B.5) $(2\nu_1 + l_1 + 2\nu_2 + l_2) = (2N + L + 2n + 1)$.

Moreover, from the orthogonality of the angular momentum eigenstates, $\bar{L}' = \bar{L}$; $\bar{M}' = \bar{M}$. In fact, we assert that the Talmi coefficients are independent of the magnetic quantum number, $\bar{M}$.

To see the latter point, it is convenient to choose $\underline{r}_1$ and $\underline{r}_2$ to be parallel. Making this assumption, and noting that,

$$\sum_{m_1,m_2} \langle l_1 l_2 m_1 m_2 | \bar{L}\bar{M} \rangle Y_{l_1}^{m_1}(\Omega)\, Y_{l_2}^{m_2}(\Omega) =$$

$$\sqrt{\frac{(2l_1+1)(2l_2+1)}{4\pi\,(2\bar{L}+1)}}\, \langle l_1 l_2 00 | \bar{L}0 \rangle\, Y_{\bar{L}}^{\bar{M}}(\Omega) \ ,$$

Eq. (B.2) can be written as,

(B.6) $$\phi_{l_1 l_1\, 2 l_2}^{\bar{L}\bar{M}}(\underline{r}_1, \underline{r}_2, b) = \psi_{\nu_1 l_1}(r_1, b)\psi_{\nu_2 l_2}(r_2, b)$$

$$\cdots \sqrt{\frac{(2l_1+1)(2l_2+1)}{4\pi\,(2\bar{L}+1)}}\, \langle l_1 l_2 00 | \bar{L}0 \rangle\, Y_{\bar{L}}^{\bar{M}}(\Omega) \ ,$$

and Eq. (B.3) can be written as,

(B.7) $$\phi_{NLnl}^{\bar{L}\bar{M}}(\underline{R}, \underline{r}, C, c) = \psi_{NL}(R, C)\, \psi_{nl}(r, c) \sqrt{\frac{(2\bar{L}+1)(2l+1)}{4\pi\,(2\bar{L}+1)}}$$

$$\cdots \langle L l 00 | \bar{L}0 \rangle\, Y_{\bar{L}}^{\bar{M}}(\Omega) \ .$$

Noting the linear independence of the spherical harmonics, Eq. (B.4) can be written as,

(B.8) i) $$\psi_{\nu_1 l_1}(r_1, b)\psi_{\nu_2 l_2}(r_2, b) \sqrt{(2l_1+1)(2l_2+1)}$$

$$\cdots \langle l_1 l_2 00 | \bar{L}0 \rangle =$$

$$\cdots \sum_{\substack{N,L \\ n,l}} \langle NLnl; \bar{L}\bar{M} | \nu_1 l_1 \nu_2 l_2; \bar{L}\bar{M} \rangle \psi_{NL}(R, C)\, \psi_{nl}(r, c)$$

$$\cdots \sqrt{(2L+1)(2l+1)}\, \langle L l 00 | \bar{L}0 \rangle \ ;$$

ii) $$\psi_{NL}(R,C)\psi_{nl}(r,c)\sqrt{(2L+1)(2l+1)}\,\langle Ll00|\bar{L}0\rangle =$$
$$\cdots \sum_{\substack{\nu_1,l_1\\ \nu_2,l_2}} \langle \nu_1 l_1 \nu_2 l_2;\bar{L}|NLnl;\bar{L}\rangle \psi_{\nu_1 l_1}(r_1,b)$$
$$\cdots \psi_{\nu_2 l_2}(r_2,b)\sqrt{(2l_1+1)(2l_2+1)}\,\langle l_1 l_2 00|\bar{L}0\rangle .$$

It is seen that the Talmi coefficients are, indeed, independent of the magnetic quantum number, $\bar{M}$; we will henceforth denote them by $\langle NLnl;\bar{L}|\nu_1 l_1 \nu_2 l_2;\bar{L}\rangle$ and $\langle \nu_1 l_1\, 2 l_2;\bar{L}|NLnl;\bar{L}\rangle$.

For the purposes of this thesis, only the Talmi coefficients of the form, $\langle N0n0;0|\nu_1 l_1 \nu_1 l_1;0\rangle$ will be required. Taking $\bar{L}$ to be zero in Eq. (B.8) i),

(B.9) $$\psi_{\nu_1 l_1}(r_1,b)\psi_{\nu_1 l_1}(r_2,b)\,(2l_1+1)\,\langle l_1 l_1 00|00\rangle =$$
$$\cdots \sum_{\substack{N,n,\\ L}} \langle NLnL;0|\nu_1 l_1 \nu_1 l_1;0\rangle\, \psi_{N0}(R,C)\psi_{n0}(r,c)$$
$$\cdots (2L+1)\,\langle LL00|00\rangle .$$

Now,

(B.10) $$\psi_{\nu_1 l_1}(r_1,b)\psi_{\nu_1 l_1}(r_2,b)\,(2l_1+1)\,\langle l_1 l_1 00|00\rangle =$$
$$\cdots = \sqrt{2l_1+1}\;\frac{2\nu_1! b^{3/2}}{(\nu_1+l_1+\frac{1}{2})!}\; e^{-\frac{b}{2}(2R^2+r^2/2)}$$
$$\cdots \sum_{j=0}^{\nu_1}\sum_{k=0}^{\nu_1}\sum_{p=0}^{2j+l_1}\sum_{q=0}^{2k+l_1} \binom{\nu_1+l_1+\frac{1}{2}}{\nu_1-j}\binom{\nu_1+l_1+\frac{1}{2}}{\nu_1-k}\binom{2j+l_1}{p}$$
$$\cdots \binom{2k+l_1}{q}\;\frac{(-1)^{j+k-q}}{j!k!}\; b^{j+k+l_1}\; r^{2(j+k+l_1)-(p+q)}$$
$$\cdots R^{p+q} ,$$

and,

(B.11) $$\sum_{\substack{N,n,\\ L}} \langle NLnL;0|\nu_1 l_1 \nu_1 l_1;0\rangle \psi_{N0}(R,2b)\,\psi_{n0}(r,\tfrac{1}{2}b)$$
$$\cdots (2L+1)\,\langle LL00|00\rangle =$$

$$\cdots = \sum_{\substack{N,n,\\ L}} \langle NLnL;0|\nu_1 l_1 \nu_1 l_1;0\rangle \sqrt{2L+1}\sqrt{\frac{4N!n!(2b\cdot\frac{1}{2}b)^{3/2}}{(N+L+\frac{1}{2})!(N+L+\frac{1}{2})!}}$$

$$\cdots e^{-\frac{(2b)}{2}R^2} e^{-\frac{(\frac{1}{2}b)}{2}r^2} \sum_{s=0}^{N}\sum_{t=0}^{n}\binom{N+L+\frac{1}{2}}{N-s}\binom{n+L+\frac{1}{2}}{n-t}$$

$$\cdots \frac{(-1)^{s\ t}}{s!t!} (2b)^{s+\frac{1}{2}L} (\tfrac{1}{2}b)^{t+\frac{1}{2}L} r^{2t+L} R^{2s+L} ,$$

whence (eliminating common factors) Eq. (B.9) can be written in the form,

$$(B.12)\ \sqrt{2l_1+1}\ \frac{2\nu_1!}{(\nu_1+l_1+\frac{1}{2})!} \sum_{j=0}^{\nu_1}\sum_{k=0}^{\nu_1}\sum_{p=0}^{2j+l_1}\sum_{q=0}^{2k+l_1}\binom{\nu_1+l_1+\frac{1}{2}}{\nu_1-j}$$

$$\cdots \binom{\nu_1+l_1+\frac{1}{2}}{\nu_1-k}\binom{2j+l_1}{p}\binom{2k+l_1}{q}\frac{(-1)^{j+k-q}}{j!k!} b^{j+k+l_1}$$

$$\cdots r^{2(j+k+l_1)-(p+q)} R^{p+q} =$$

$$\sum_{\substack{N,n,\\ L}} \sqrt{2L+1}\sqrt{\frac{4N!n!}{(N+L+\frac{1}{2})!\,(n+L+\frac{1}{2})!}} \sum_{s=0}^{N}\sum_{t=0}^{n}\binom{N+L+\frac{1}{2}}{N-s}$$

$$\cdots \binom{n+L+\frac{1}{2}}{n-t}\frac{(-1)}{s!t!} b^{s+t+L} 2^{s-t} r^{2t+L} R^{2s+L} .$$

A recursive formula for the required Talmi coefficients can be found by equating the coefficients of the monomials, r^0R^{2s}, in Eq. (B.12). For these coefficients:

$L= t=0;\quad p\ q=s;\quad j+k+l_1=s;\quad p=2j+l_1;\quad q=2k+l_1$;

and we obtain the relation,

$$(B.13)\quad \sqrt{2l_1+1}\ \frac{2\nu_1!}{(\nu_1+l_1+\frac{1}{2})!} \sum_{\substack{j+k+l_1=s\\ j,k\le\nu_1}} \binom{\nu_1+l_1+\frac{1}{2}}{\nu_1-j}\binom{\nu_1+l_1+\frac{1}{2}}{\nu_1-k}\frac{1}{j!k!}$$

$$= \sum_{\substack{N+n=N_m\\ N\ge s}} \langle N0n0;0|\nu_1 l_1 \nu_1 l_1;0\rangle \sqrt{\frac{4N!n!}{(N+\frac{1}{2})!(n+\frac{1}{2})!}}\binom{N+\frac{1}{2}}{n-s}$$

$$\cdots \binom{n+\frac{1}{2}}{n}\frac{2^s}{s!} .$$

where,

$$N_m \equiv 2\nu_1 + l_1 + 2\nu_1 + l_1 \quad .$$

From Eq. (B.13), it is straightforward to show that,

$$(B.14)\quad \langle s0(N_m-s)0;0|\nu_1 l_1 \nu_1 l_1;0\rangle =$$

$$\sqrt{\frac{s!(N_m-s)!(s\ \frac{1}{2})!}{(N_m-s\ \frac{1}{2})!}}\quad (\tfrac{1}{2}!)\ \Bigg[2^{-s}\sqrt{2l_1+1}\ \nu_1!$$

$$\cdots\ (\nu_1+l_1+\tfrac{1}{2})!\quad \sum_{\substack{j+k+l_1=s \\ j,k\leq\nu_1}} (\nu_1-j)!\,(\nu_1-k)!$$

$$\cdots\ (j+l_1+\tfrac{1}{2})!\,(k+l_1+\tfrac{1}{2})!\,j!\,k!\Bigg]^{-1} -$$

$$\cdots - \sum_{N=s\ 1}^{N_m} \langle N0(N_m-N)0;0|\nu_1 l_1 \nu_1 l_1;0\rangle$$

$$\cdots\sqrt{\frac{N!(N+\frac{1}{2})!(n+\frac{1}{2})!}{n!}}\quad \left[(N-s)!\,(s+\tfrac{1}{2})!\,s!\,\tfrac{1}{2}!\right]^{-1} .$$

The Talmi coefficients employed in this thesis have been evaluated from the recursive formula, Eq. (B.14).

APPENDIX C CALCULATION OF THE ONE-BODY DIFFERENTIAL ELASTIC SCATTERING CROSS-SECTION

In this appendix, we derive the s-wave differential elastic scattering cross-section for the scattering of a particle from a spherical one-body potential. The approach which is adopted is to express the cross-section in terms of the logarithmic derivative of the resonant one-body wave function. This general method of approach is familiar from the R-matrix theory of nuclear reactions, the present case being, perhaps, the simplest example.

We take the one-body Schroedinger equation to be,

$$(C.1)\quad \left[-\frac{\hbar^2}{2\mu}\nabla^2 + \frac{ZZ'e^2}{R} + V(R)\right]\phi(R) = \epsilon\phi(R) ,$$

where μ is the reduced mass of the one-body system; Ze and Z'e are the charges of the two interacting particles. Here,

$$(C.2)\quad V(R) = V_C(R) - \frac{ZZ'e^2}{R} + V_N(R) ,$$

where $V_C(R)$ and $V_N(R)$ are the one-body electrostatic and nuclear potentials, respectively. Due to the short range of the nuclear force, V(R) is typically a short-range potential. The scattering cross-section from such a potential is well-known (Messiah (1962)):

$$(C.3)\quad \sigma(\theta) = |f(\theta)|^2 ,$$

where,

$$(C.4)\quad f(\theta) = -\frac{\eta}{2k\sin^2\frac{1}{2}\theta}\,\mathrm{EXP}(-i\eta\ln(\sin^2\tfrac{1}{2}\theta) + 2i\sigma_0) \cdots$$

$$\cdots \frac{1}{2ik}\sum_{l=0}^{\infty}(2l+1)\,e^{2i\sigma_l}\,(e^{2i\delta_l} - 1)P_l(\cos\theta) .$$

Here,

$$(C.5)\quad i)\quad k = \frac{\sqrt{2\mu\epsilon}}{\hbar} ;$$

ii) $\eta = \frac{ZZ'e^2}{\hbar}\sqrt{\frac{\mu}{2\epsilon}}$;

iii) $\sigma_l = \arg\Gamma(l+1+i\eta)$;

and δ_l is the phase shift of the l^{th} partial wave. Defining,

(C.6) i) $\beta = \eta \ln(\sin^2\frac{1}{2}\theta)$;

ii) $\gamma = \frac{\eta}{\sin^2\frac{1}{2}\theta}$;

and neglecting contributions to the cross-section from all partial waves other than s-waves ($l = 0$), Eq. (C.3) becomes,

$$(C.7)\quad \sigma(\theta) = \frac{\gamma^2}{4k^2} - \frac{\gamma}{k^2}\cos(\beta+\delta_0)\sin\delta_0 + \frac{\sin^2\delta_0}{k^2} \quad .$$

It is seen from Eq. (C.7) that, to evaluate the differential elastic scattering cross-section, we need only evaluate the phase shift, δ_0. The phase shift is defined by the asymptotic property,

$$(C.8)\quad u_0(R) \sim A\left[(G_0 - iF_0) - e^{2i\delta_0}(G_0 + iF_0)\right] \quad ,$$

which holds since $V(R)$ is a short-range force. Here, F_0 and G_0 are the regular and irregular Coulomb functions of zero angular momentum; $u_0(R)$ is the radial part of the zeroth partial wave solution of Eq. (C.1), being a solution of the radial Schroedinger equation,

$$(C.9)\quad -\frac{\hbar^2}{2\mu}\frac{d^2u_0}{dR^2} + \left[\frac{ZZ'e^2}{R} + V(R)\right]u_0 = \epsilon_0 u_0 \quad .$$

It is convenient to define the $\mathcal{R}$ function to be,

$$(C.10)\quad \mathcal{R}_0 = \left.\frac{u_0(R)}{R\frac{du_0(R)}{dR}}\right|_{R=R_0} \quad ,$$

where R_0 is a suitably large radius. It is then easily shown that,

$$(C.11)\quad \delta_{0(\epsilon')} = \tan^{-1}\left[\frac{RF_0'(R,\epsilon') - F_0(R,\epsilon')/\mathcal{R}}{G_0(R,\epsilon')/\mathcal{R} - RG_0'(R,\epsilon')}\right]_{R=R_0} \quad ,$$

Noting the Wronskian relation,

$$(C.12)\quad F_o' G_o = G_o' F_o + k \quad ,$$

Eq. (C.11) can be written as,

$$(C.13)\quad \delta_o(\epsilon') = \tan^{-1}\left[\frac{kR}{G_o^2\left(\frac{1}{R} - R\frac{G_o'}{G_o}\right)} - \frac{F_o}{G_o}\right]_{\substack{R=R_o \\ \epsilon=\epsilon'}} .$$

The cross-section in section 4 - 2 of this thesis was plotted by numerically evaluating the logarithmic derivative of the one-body wave function of Eq. (C.9) about resonance. The phase shift was then found from Eq. (C.13), and the cross-section from Eq. (C.7).

The width of the cross-section can be obtained from the Breit-Wigner one-level formula; a discussion of the one-level approximation can be found in the book by Preston (1962). It can be shown from the formulas for the scattering cross-section stated by Preston that,

$$(C.14)\quad \sigma(\theta) = \frac{\gamma^2}{4k^2} - \frac{\gamma}{k^2}\cos(\beta + D_o)\sin D_o + \frac{\sin^2 D_o}{k^2} \quad ,$$

where,

$$(C.15)\quad \text{i)}\ \sin^2 D_o = \frac{B^2/4}{(\epsilon - \epsilon_o)^2 + B^2/4} \quad ;$$

$$\text{ii)}\quad B = \frac{\Gamma}{1 - \frac{d\Delta}{d\epsilon}\Big|_{\epsilon=\epsilon_o}} \quad .$$

Here, Γ is the width of the scattering cross-section; ϵ_o is the resonance energy;

$$(C.16)\quad \Delta = -S_o \gamma^2$$

is the level shift (S_o being the shift function and γ^2 the one-body reduced width). By comparing Eqs. (C.7) and (C.11), it

is seen that we may identify D_0 with the phase shift, δ_0. The coefficient, B, can then be found from Eq. (C.15) i) by making a least squares fit to the phase shift, δ_0.

To evaluate the width of the scattering cross-section from Eq. (C.15) ii), we require the energy dependence of the level shift. For heavy nuclei, where there are large Coulomb barriers, this energy dependence is given to good approximation by,

$$(C.17) \quad \frac{d\Delta}{d\epsilon} = -\rho\gamma^2 \left[\frac{1}{2\epsilon} \frac{\dot{G}_0}{G_0} + \frac{d}{d\epsilon}\left(\frac{\dot{G}_0}{G_0}\right) \right]_{R=R_0} . \quad (\rho = kR, \ \dot{G}_0 = \frac{dG_0}{d\rho})$$

In this thesis, the effect of the energy dependence of the level shift has been estimated from Eq. (C.17) by calculating the energy dependence of G_0.